



VICTORIA UNIVERSITY
MELBOURNE AUSTRALIA

Effect of uniaxial loading on the spalling of concrete panels for Melbourne's Metro Tunnel Project

This is the Published version of the following publication

Guerrieri, Maurice, Lee, Duffy, Lee, Vern and Haines, Luke (2024) Effect of uniaxial loading on the spalling of concrete panels for Melbourne's Metro Tunnel Project. *Structural Concrete*, 25 (3). pp. 1676-1701. ISSN 1464-4177

The publisher's official version can be found at
<https://onlinelibrary.wiley.com/doi/10.1002/suco.202200556>
Note that access to this version may require subscription.

Downloaded from VU Research Repository <https://vuir.vu.edu.au/48592/>

ARTICLE

Effect of uniaxial loading on the spalling of concrete panels for Melbourne's Metro Tunnel Project

Maurice Guerrieri¹  | Duffy Lee² | Vern Lee³ | Luke Haines⁴

¹Institute of Sustainable Industries & Liveable Cities (ISILC), Victoria University, Melbourne, Victoria, Australia

²Gamuda Australia, Sydney, New South Wales, Australia

³Love Reinforcing, Braybrook, Victoria, Australia

⁴Risconsult, Perth, Western Australia, Australia

Correspondence

Maurice Guerrieri, Institute of Sustainable Industries & Liveable Cities (ISILC), Victoria University, Melbourne, Victoria, Australia.

Email: maurice.guerrieri@vu.edu.au

Abstract

The Metro Tunnel is a Victorian Government funded infrastructure project which will create a new end-to-end rail line from Sunbury in the west to Cranbourne/Pakenham in the south east, with bigger and better trains, next generation signaling technology and five new underground stations. This article provides a detailed summary of the structural fire testing requirements for the platform tunnel side wall and arch lining in the Metro Tunnel's State Library and Town Hall stations. Contrasted to building fires, tunnel fires are more significant within a few minutes due to the confined space which can cause concrete spalling and jeopardize the bearing capacity of the tunnel, which is a significant concern to designers. The catastrophic European tunnel fire events in 1999 and 2001 led to the development of innovative regulations and recommendations, including guidelines endorsed by the European Federation of National (EFNARC 132F r3:2006) and Efectis R0695:2020. This paper explains the methodology taken to design the fire rated concrete test for the platform tunnel side wall and arch lining in the State Library and Town Hall stations of Melbourne's Metro Tunnel Project for structural stability for the period of a serious fire event. For the first time, uniaxial loading (500T) was applied to five large-scale flat concrete panels (1800 × 1800 × 400 mm) which are normally unloaded during fire exposure and exposed to the RABT ZTV (rail) fire curve. The first testing program investigated the influence of polypropylene dosage in the concrete mix design and its effect on the magnitude and severity of concrete spalling. The results indicated that the recommended 2.0 kg/m³ polypropylene dosage requirement as specified by Eurocode is conservative. Concrete mix designs with a stable aggregate and the correct curing regime can mitigate spalling at significantly lower polypropylene dosage rates. The water pooling effect was evident during the fire testing and the surface cracking that developed was vertical to the surface, allowing for the release of the pore water pressure build-up.

KEYWORDS

concrete, fire resistance, polypropylene fibers, spalling, tunnel fire, uniaxial loading

This is an open access article under the terms of the [Creative Commons Attribution](https://creativecommons.org/licenses/by/4.0/) License, which permits use, distribution and reproduction in any medium, provided the original work is properly cited.

© 2024 The Authors. *Structural Concrete* published by John Wiley & Sons Ltd on behalf of International Federation for Structural Concrete.

1 | INTRODUCTION

Several devastating tunnel fire incidents have happened over the past 30 years, including the Channel Tunnel (England-France) in 1996, Mount Blanc Tunnel (France-Italy) in 1999, and the St. Gothard Tunnel (Switzerland) in 2001.¹ In 2005, a fire broke out during construction in the Shanghai Metro Line 8 tunnel, which initiated concrete spalling alongside the 16.8 m tunnel lining segments (up to 25 mm in depth). The fire also threatened the joint seal, which could have caused flooding of the tunnel given the tunnel was built under the water level and was surrounded by soft ground with high water pressure.² In 2007, a fire broke out in the Burnley Tunnel, Melbourne, Australia, caused by a rear-end collision involving three lorries and four cars. The tunnel is a 3.4 km long road tunnel with its deepest point, 60 m below sea level. Three fatalities resulted and the tunnel's deluge system quickly extinguished the fire with no reports of concrete spalling or structural damage. Table 1 provides a detailed summary of tunnel road and rail fires around the world and the reader is referred to the works of Beard and Carvel⁴ for a detailed summary. Hua et al.⁵ provides a framework to quantify damage during a passenger train tunnel fire event, by considering uncertainties within the fire event and quantifying these parameters using a simplified model for damage assessment. This paper provides the experimental analysis for large-scale testing of a real life passenger train tunnel.

Lessons from past accidents have led to the development of stricter practices assigned by different authorities and various research activities.⁶ These incidents have led to requirements in limiting the spalling depth and the magnitude of temperatures of the *in situ* reinforcement⁷ for both rail and road tunnels. Throughout the previous decade, the quantity of underground tunnels has significantly increased globally⁸ and as a result of COVID-19 Australia, like many countries, are fast tracking tunnel transportation projects to revitalize the economy. This has necessitated the need to evaluate the impacts of fire within the tunnel on the tunnel lining itself and the adjacent surrounding area in greater detail. This is of specific significance for tunnels constructed in urban areas where above- and below-ground assemblies can be exceptionally vulnerable to surrounding ground deformations and groundwater level fluctuations.⁸ Whilst fires in road tunnels are more common, there are more fatalities associated with rail tunnel fires.^{4,9,10}

Separately from fatalities and injuries, losses associated with property and lengthy interruptions of operations and services may arise, if there is significant damage to the tunnel lining. In the event of the Channel Tunnel Fire of 1996, the fire caused the nominal 450 mm

tunnel lining thickness to reduce to 100–200 mm,¹¹ which needed more than 1300 t of fiber-reinforced shotcrete for restoration. This caused the tunnel to be closed for almost 6 months, resulting in approximately \$1.5 M in uncollected tolls.⁹

Explosive spalling of concrete can be best described as an extreme showering of heated sections of concrete that can affect firefighting service personnel, making their work significantly more challenging and hazardous.^{12,13} This type of spalling can lead to the failure of concrete layers, commonly reaching thicknesses between 25 and 100 mm, varying on each specific case.¹⁴ Jansson¹⁵ recounted that the works of Barret¹⁶ in 1854 were the first time recorded observation of concrete spalling was made. The researched showed that when the aggregate used to manufacture concrete was flint, the concrete was said to have split and yielded when it was exposed to fire. Another phenomenon commonly associated with fire testing of concrete panels is the egress of water from the unexposed surface, also known as water pooling, which was first recorded in 1905 by Woolson.¹⁷ It has been shown that this phenomenon occurs even on 300 mm full-scale structural loaded tunnel segments exposed to fire on the underside,¹⁸ similar to the findings of Jansson.¹⁵

The most effective way to significantly reduce the probability of spalling is to accurately design the concrete mix taking into account the performance of the aggregate and ensure that is stable^{19,20} combined with incorporating pozzolan cements such as fly ash and slag, which have proven to reduce the probability of spalling.^{21–24} The addition of polypropylene fibers has proven to reduce spalling when employed at the proper dosages provided the aggregate is stable.^{25–27} A very recent study by McNamee et al.²⁸ has shown that the recommended polypropylene dosages recommended by Eurocode 2²⁹ of $>2 \text{ kg/m}^3$ are conservative and that the spalling behavior can be reduced by on average 50% across 26 samples when the polypropylene dosage was reduced to 0.2 kg/m^3 .

Liu et al.²⁶ showed that throughout heating, the microfibers melt, causing an improvement in connectivity of isolated pores and an increase in gas permeability. Additionally, polypropylene fibers cause the development of microcorridors when the concrete is heated lessening the impact of the moisture clog, which considerably increases the likely hood of spalling.²⁵ For a state-of-the-art analysis of the theory of how polypropylene fibers work and general theories linked to concrete spalling including ahistorical review, the reader is referred to the workings of Jansson¹⁵ and McNamee.³⁰

No accurate theoretical methods exist to predict concrete spalling due to fire exposure, consequently

TABLE 1 Summary of major tunnel fire. Modified from ref.³

Year	Tunnel location	Accident type	Casualties	Comments
1949	Holland tunnel-United States	Load falling off lorry explosion	66	Serious damage to structure over 1100 m
1968	Moorfleet-Germany	Car accident	-	Serious damage on vault and side wall
1972	Hokuriku tunnel-Japan	Short circuit	744	No extinguishers and no exhaust way to release smoke
1974	Mont Blanc tunnel France-Italy	Motor fire	1	-
1975	Guaderrama tunnel-Spain	Truck fire	-	Serious damage to structure
1976	Crossing BP—A6-France	Lorry fire	12	Serious damage over 150 m
1978	Velsen tunnel-Netherland	Collision	10	Serious damage over 30 m
1979	Nihonzaka Tunnel-Japan	Collision	8	Serious damage over 1100 m
1980	Kajiwara-Japan	Collision with side wall	1	Serious damage over 1100 m
1980	Sakai-Japan	Collision	10	Serious damage to structure
1982	Caldecott-United States	Collision	9	Serious damage over 580 m
1982	Salang tunnel-Mazar-eSharif-Kabul Afghanistan	Probably mine explosion	2700–3000	-
1983	Pecrile-Italy	Collision	31	-
1983	Frejus-France-Italy	Motor fire	-	Damage to roof slab and equipment
1984	Gotthard tunnel-Switzerland	Motor fire	-	Serious damage over 30 m
1984	Summit tunnel fire-England	Train derailed	-	Thirteen tankers containing petrol caught fire and the fire took 4 days
1984	Felbertauern tunnel-Austria	Blocking brakes	-	Damage to pavement and ceiling
1984	San Benedetto tunnel-Italy	Bomb attack	137	Railway tunnel
1986	L'Arme-France	Collision	8	-
1987	Gumefens-Switzerland	Collision	2	-
1990	Roldal tunnel-Norway	Motor fire	1	-
1990	Mont Blanc tunnel-France-Italy	Motor fire	2	Some equipment destroyed
1993	Serra Ripoli Tunnel-Italy	Collision	8	-
1993	Hovden-Norway	Collision	5	111 m insulation material destroyed
1994	Hugouenot-South Africa	Electrical fault	29	Serious damage on tunnel lining
1994	Great Belt-Denmark	Construction turnover	-	Widespread damage on tunnel region
1995	Pfander Tunnel-Austria	Collision	7	Serious damage to structure
1995	Baku underground railway-Azerbaijan	Electrical malfunction	559	-
1996	Channel Tunnel-Britain-France	Cargo fire	2	Widespread damage on tunnel region
1996	Isola delle Femmine-Italy	Collision	25	Serious damage tunnel and closed for 2.5 days
1999	Mont Blanc-France-Italy	Oil leakage motor	39	Serious spalling on tunnel lining
1999	Tauren Tunnel-Austria	Multi-car collision	61	Serious damage to structure and part of tunnel vault collapsed
2000	Seljestad tunnel-Norway	Multi-car collision	6	Serious damage to structure and tunnel closed for 1.5 days.
2000	Gletscherbahn Kaprun-Austria	Electric fan heater	155	Fire had burned through a 16 kW power cable
2001	Gothard-Switzerland	Two trucks collision	21	Serious spalling on tunnel lining
2001	Gleinalm tunnel-Austria	Collision	9	Tunnel structures was seriously damaged
2001	Prapontin tunnel-Italy	Spontaneous combustion of tire	11	-

TABLE 1 (Continued)

Year	Tunnel location	Accident type	Casualties	Comments
2001	Madaoling Tunnel-China	Engine fire	18	-
2002	A86 Road Tunnel-France	Construction turnover	-	Surface concrete damage
2002	Roppener Tunnel-Austria	Motor fire	2	-
2002	Homer tunnel-New Zealand	-	4	-
2002	Maoliling Tunnel-China	Engine fire	-	Caused great economic losses and interrupted traffic 18 days
2003	Vicenza-Italy	Bus turnover	56	-
2003	Daegu subway-South Korea	Subway fire	340	Rapid spread of flames and smoke due to petrol incendiary incidents
2003	Shidaoshan tunnel-China	Spontaneous combustion	-	-
2003	Baregg Tunnel-Switzerland	Collision	6	-
2004	Takayama-Japan	Collision	5	Surface concrete damage
2004	Niuguantou tunnel-China	Spontaneous combustion	-	-
2005	Frejus-France-Italy	Car accident	23	Serious damage on tunnel lining
2005	Feiluanling tunnel-China	Passenger car brake failure	8	-
2006	Viamala-Switzerland	Car-bus collision	15	-
2006	Wenquan Tunnel-China	Truck tire burst into flames	-	Facilities were severely damaged
2007	Burnley Tunnel-Australia	Collision	3	-
2007	San martino-Italy	Collision and fire	12	-
2007	Chongqing University city tunnel-China	Technical problems	6	Lighting and ventilation system are paralyzed
2007	Newhall Pass tunnel-United States	Multi-truck collision	13	It took 24 h to control the fire and structure was severely damaged
2008	Ofenauer-Austria	Collision	17	-
2008	Dabaoshan Tunnel-China	Collision and fire	2	-
2009	Gubrist-Switzerland	Collision and fire	4	-
2009	Arlberg-Austria	Collision	3	-
2009	Qinling zhongnanshan tunnel-China	Truck carrying burning quilt	-	-
2009	Eiksund Tunnel-Norway	Collision	5	-
2010	Huishan Tunnel-China	Man-made arson	43	Damage on mechanical and electrical facilities
2011	Xinqidaoliang-China	Shunt	5	Widespread damage on tunnel region
2012	Xueshan Tunnel-China	Collision and fire	24	-
2013	Liushiliang Tunnel-China	Multi-car collision	18	Damage on tunnel facilities
2014	Yanhou-China	Collision	31	Serious damage on tunnel lining
2015	Fenghuangshan tunnel-China	Collision and fire	-	-
2016	Mangshan tunnel-China	Collision and fire	1	-
2017	Taojiakuang tunnel-China	Arson	11	-
2018	San Bernardino-Switzerland	Bus crash	-	Caused longest traffic jam in 19 years
2018	Detroit-Windsor tunnel	Collision	1	Tunnel temporarily closed

(Continues)

TABLE 1 (Continued)

Year	Tunnel location	Accident type	Casualties	Comments
2019	Maoliling Tunnel-China	Spontaneous combustion of tire	36	-
2019	Rannersdorf tunnel-Austria	Trailer-tractor	-	Wiring and concrete ruptured in the ceiling
2020	Central Park North-110th Street station-United States	Possible arson	17	Severely damaged the north part of the station and the train cars
2020	Samae 2 Tunnel-Korea	Collision and fire	47	Tank truck carrying nitric acid ran into some cars involved in an earlier accident
2020	Sydney Harbor Tunnel-Australia	-	-	Hundreds of people were stuck inside tunnel

evaluation is typically completed through fire tests, however, limited facilities exist worldwide. These tests are essential to be conducted on a large scale to reproduce the identical boundary conditions, stress conditions, and material properties of the real structure, all of which are dependent on the spalling behavior.

Limited large-scale experimental studies have been carried out on the performance of tunnel linings in fire^{7,31–39} including the Runehamar fire tests.⁴⁰ Nevertheless, only limited works^{7,18,31,33,37,39} have been conducted on full-scale tunnel lining segments that were tested under combined structural and fire loading. These tests included real life boundary conditions, external loading, and conditioning comparable to design expectations. Whilst many tests have been conducted on unloaded flat panels in accordance with EFNARC 132F r3:2006,⁴¹ only limited works have been tested on flat panels under uniaxial loading and often on small-scale slabs^{42–47} apart from the only study by Parwani et al.⁴⁴ who carried out uniaxial testing on full-scale concrete panels in accordance to Efectis R0695:2020.⁴⁸ Table 2 presents a summary of these tests. Hua et al.⁵ also provides a detailed summary of recent fire tests on tunnel segments/slabs. This paper presents an overview of the methodology taken to design the large-scale concrete fire test in relation to the platform tunnel side wall and arch lining in the Metro Tunnel Project's State Library and Town Hall stations for structural stability in case of a serious fire event such as the RABT ZTV (rail) fire scenario. Details of the test program and results will be presented and discussed.

2 | PROJECT OVERVIEW

The Metro Tunnel venture located in Melbourne incorporates dual 9-km rail tunnels that connect inner west Kensington through to South Yarra in the inner southeast of

Melbourne.¹⁸ The Metro Tunnel will connect the Sunbury and Pakenham/Cranbourne lines, circumventing current congested inner city tracks as shown in Figure 1.¹⁸ Earth pressure balance tunnel boring machines (TBM) side by side with an excavation diameter of 7.28 m, segment diameter of both tunnels 6.90 m, and thickness of 0.300 m are used to construct the tunnels.¹⁸

The Metro Tunnel Project will consist of five underground stations at Anzac on St Kilda Road, Town Hall (at the southern end of Swanston Street), Arden (western end of Queensberry Street in North Melbourne), Parkville (Grattan Street and Royal Parade), and State Library (at the northern end of Swanston Street), whilst significantly increase inner city station capability and linking the Parkville and Domain precincts to the rail network for the first time.¹⁸ The twin tunnels consist of more than 56,000 precast tunnel lining segments.¹⁸





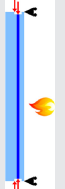
2.1 | Regulatory context

A co-regulatory structure governs rail safety regulation in Australia. The Office of Rail Safety Regulator (ONRSR) is an impartial authority created under the Rail Safety National Law (RSNL).¹⁸ The principal objective of the ONRSR is to implement secure railway operations and enhance national rail safety. ONRSR, in its recommended accompanying documentation to the RSNL⁵¹ recommends guidance on the current duty to:

- Eradicate safety hazards so far as is realistically practicable, and
- If it is not reasonably feasible to eliminate, to reduce those risks so far as is realistically practicable.

What is relatively achievable is an objective test and depends on what can be done? that is¹⁸:

TABLE 2 Summary of the state-of-the-art of fire testing of concrete flat panels.

	Hua et al. ⁴⁹	Parwanni et al. ⁴⁴	Lo Monte et al. ⁴⁵	Miah et al. ⁴⁶
Specimen size and scale, (m)	2.44 × 1.83 × 0.3	5.00 × 2.40 × 0.40	0.80 × 0.80 × 0.10	0.2 × 0.2 × 0.2 and 0.88 × 0.8 × 0.1
Compressive strength (MPa)	55	25	60	41.0–51.2
Curing and conditioning	Slabs sprayed with water and covered with canvas for the first month after casting + followed by 8 months of lab ambient condition curing.	Cured minimum 3 months	Not mentioned	24 h cured with polyethylene sheet cover until test date, >28 days
Fire curve	Up to 1000°C at a heating rate of 40°C/min.	RWS	Standard fire curve	Standard fire curve
Test methodology	Loaded by test rig	Loaded by test rig	Biaxial loaded by test rig	Uniaxial + biaxial
Schematic				
Stress applied (kN or MPa)	310 kN	10–15 MPa	10 MPa	0.4, 8, 12, 16, and 20 MPa
Measurements	<ul style="list-style-type: none"> Temperature at concrete face by thermocouples Stresses by applied load gages Vertical displacement Spalling depth 	<ul style="list-style-type: none"> Temperature at concrete face by thermocouples Not mentioned Not mentioned Time of first spalling 	<ul style="list-style-type: none"> Temperature at different depth with thermocouples Stresses by applied load gages Vertical displacement Not mentioned Spalling depth contour map 	<ul style="list-style-type: none"> Temperature at different depth with thermocouples Stresses by applied load gages Not mentioned Spalling depth contour map
Specimen size and scale, (m)	0.50 × 1.00 × 0.20, 2.00 × 2.60 × 0.40	1.425 × 1.25 × (0.15–0.70)	580 × 680 × 150	0.40 × 0.40 × 0.1, 3.60 × 0.60 × 0.20, 1.80 × 1.20 × 0.40
Compressive strength (MPa)	48	30–75.3	37	72.9–106.9
Curing and conditioning	Not mentioned	3 months after poured	Demold after 24 h. 23°C and 100% RH for 28 days.	Cured with covered by plastic foil conditioned under water @20°C. Removed from water thank 1 week before test
Fire curve	RABT	Increased hydrocarbon	ISO-834	ISO 834
Test methodology	Loaded by posttensioning and hydraulic jacks	Slabs are hanging on support beams	Slabs are hanging on support beams	Flat—prestress loaded, bending by eccentric place wires
Schematic				

(Continues)

TABLE 2 (Continued)

	Kato et al. ⁴³	Tailefer et al. ⁵⁰	Carre et al. ⁴⁷	Bostrom et al. ⁴²
Stress applied (MPa)	14	Unloaded	5, 10, 15	0–8.8
Measurements				
• Temperature	Temperature at different depths	Temperature at different depths	Temperature at different depths + pore pressures	Not mentioned
• Stress	Not mentioned	Not mentioned	Not mentioned	Not mentioned
• Displacement	Not mentioned	Not mentioned	Not mentioned	Deformation measurement
• Spalling	Contour maps	Zone mapping	Contour maps	Weighing and depth of the scaled off material by sliding caliper

- What is feasible in the situations?
- Whether it is acceptable, in the circumstances, to do all that is feasible?
- After assessing the risk, the available ways of eliminating or minimizing the risk and the associated costs, whether the cost sustained is grossly disproportionate to the risk benefit gained.

The ONRSR advises the use of preventative methodology in the challenges of uncertainty that is, presume that safety measures should be commenced unless there is a convincing case not to take them.

2.2 | Why tunnel concrete fire testing?

Road tunnels are commonly installed with some system of water-based suppression, unlike rail tunnels due to risks associated with electrocution. In most rail tunnels, there is no automated suppression system in the tunnel or on the rolling stock.¹⁸ The main fire defense approach implemented is controlling the materials used in the tunnels and passenger rolling stock that have passed critical fire materials testing. This is required to reduce the likelihood of fire ignition and in the event of ignition reduce the likelihood that a fire will grow to a significant size.

It is not practical to completely eliminate the risk of a fire in a tunnel as the tunnel vehicles including cars, passenger train itself, maintenance vehicles (e.g., rail grinders), diesel locomotives, and so forth, pose a risk of large fire within the tunnel.¹⁸ Due to the difficulty of the fire brigade response in accessing the fire location in a tunnel due to the presence of trapped vehicles and high voltage equipment,¹⁸ it is critical for the tunnel structure to be designed and constructed to achieve the desired structural fire performance objectives. The most important objective for tunnel operators is to move people quickly and safely in the event of a tunnel fire. Secondary objectives are to minimize any damage to the tunnel to maintain operation and minimize disruptions and costs associated with repair. To minimize major structural damage during a tunnel fire whilst ensuring the regulations and regulators expectations are met, structural concrete fire tests are carried out to assure the fire performance of the tunnel under agreed realistic fire scenarios.¹⁸

3 | TESTING PROGRAM

3.1 | Fire load analysis

The project scope and Technical Requirements (PS&TR) defines two different requirements for fire resistance of



FIGURE 1 Metro Tunnel Project alignment, Melbourne (modified from Guerrieri et al.¹⁸).

primary structural elements as (as shown in Figure 2) follows:

- Primary load bearing structural elements below ground (including cross passages, shafts, retaining walls, internal walls, beams, columns, slabs, and cavern structures) shall be structurally adequate for a 4-h standard fire curve, that is, 240/(120)/(120), as defined by the AS 1530.4⁵² time-temperature curve.
- Primary structure surrounding trackway or trackway structural elements (including TBM pre-cast segments, mined tunnel cast *in situ* linings and cavern cast *in situ* linings) shall be designed for the RABT-ZTV (rail) time-temperature curve.

For the State Library Station’s Cavern, the above requirements mean that all elements of the structure shall comply with the 4 h standard fire curve, and in addition, the cast *in situ* lining adjacent to the trackway shall also comply with the RABT-ZTV (rail) fire curve. Reinforced concrete structural elements which are subject to only the standard fire curve do not require numerical analysis, as they are deemed to comply to provisions of AS 3600,⁵³ subject to the structural element meeting the specified dimensional limits. Reinforced concrete structural elements, which are subject to both fire curves are required to be designed to meet the requirements of the two fire conditions. The

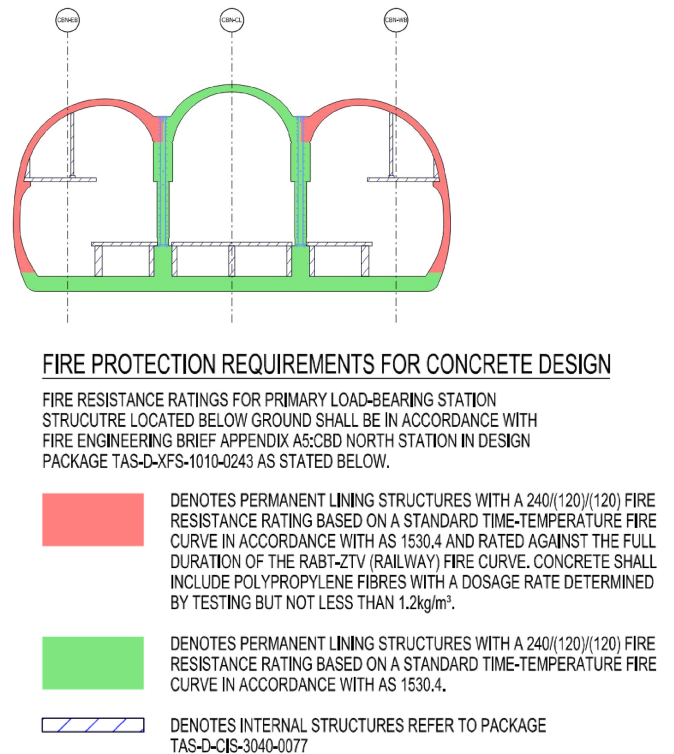


FIGURE 2 Cross-section of the CBD Trinocular Cavern.

bracketed (120) in the fire resistance rating means “if required.” For primary load bearing structural elements cast against the ground, the fire resistance rating shall

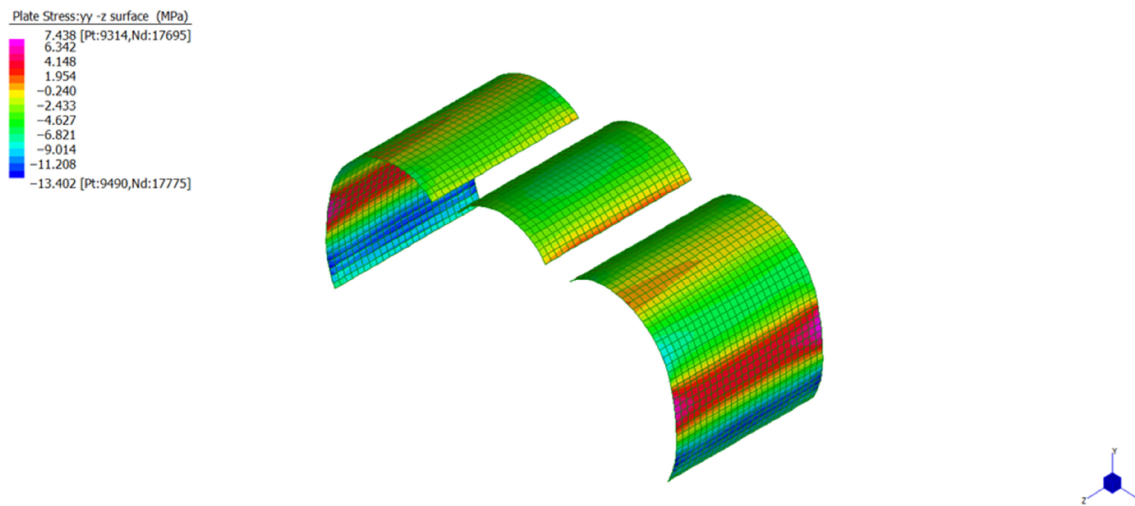


FIGURE 3 Serviceability limit state load combination 80B.

be 240/—/—, as there is no requirement for fire protection for insulation or integrity.

A comparative study (numerical analysis) has been undertaken to compare the performance under fire of a typical 450 mm thick 50 MPa concrete section (similar size to a typical station cavern lining). The comparative study compared the 4 h standard fire curve with 0 mm spall to the RABT-ZTV (rail) fire curve with 20 mm spall and concluded that for the same fixed conditions, the 4 h standard fire curve was more onerous in terms of temperature profile, loads, and deformations induced in the concrete element than the RABT-ZTV (rail) fire curve. The conclusion of the study was that any structural element, which is designed to satisfy the standard 4 h ISO fire condition (referred to the standard time temperature curve of AS1530.4⁵²) will also satisfy the structural fire resistance requirements of the RABT-ZTV (rail) fire curve.

Where primary structures are required to be designed for both fire conditions, then for a design which satisfies the standard 4 h ISO fire condition, then the structural fire resistance requirements of the RABT-ZTV (rail) fire condition will also be satisfied. Fire testing is required to confirm the spalling depth and thermal profile for the RABT-ZTV (rail) fire curve to validate the assumptions adopted for the comparative study.

To support the proposed maximum compression level of 8 MPa for the Cavern fire test panel, axial force plot along the 450 mm thick sidewall for each of the load, 80 cases are plotted to derive peak and average thrust along a 12 m length. Maximum compression level of 8 MPa has been proposed for the Cavern fire test panel. The following figures summarize the maximum serviceability limit state (SLS) stress in the typical cavern sidewall by SLS load case. The maximum stress is 7.6 MPa. An upper bound test load of 8 MPa was selected on this

basis. Some very localized stress concentrations occur in the cavern stub regions, but as these are localized, are not considered for the fire test as shown in Figure 3.

3.2 | Structural fire testing furnace arrangement

The structural fire testing furnace is outfitted with 12 gas powered burners (3GJ/h each) and the furnace is assembled in a modular format to provide the ability of testing beams, columns, floors/ceilings, ducts, and walls in both an unloaded and loaded arrangement.¹⁸ The inner sizes of the furnace are 4500 × 3700 × 3000 mm, and the furnace has the capability to run any international fire curve including clientele specific designed curves. For example, only the RABT ZTV (Train/Car) fire curves involve the furnace temperatures to achieve 1200°C and then decrease to ambient temperatures linearly.¹⁸ This linear cooling stage can be designed to be implemented when the user chooses, including at the end of a 2-h modified hydrocarbon fire test.¹⁸ The furnace is also outfitted with 12 viewing ports and a furnace endoscope providing real-time 4 k video footage of the combustion chamber. The furnace time temperature program is controlled by eight Type K (National Association of Testing Authorities [NATA] Certified up to 1350°C; 3-mm diameter, 310 stainless steel mineral insulated metal sheathed) thermocouples that are positioned in the furnace relevant to the testing standard specified.¹⁸ Whilst the furnace has been used previously for testing four unloaded flat panels simultaneously with plan dimensions of 1550 × 1550 × 260 mm and full-scale structural loaded tunnel elements as previously published,¹⁸ the furnace is also able to test panels up to 1800 × 1800 × 400 structurally loaded biaxially (up to 500 t at 50% yield) as

FIGURE 4 Schematic illustration of (a) flat panel testing assembly on top of furnace and (b) birdseye view of biaxial structural frame with specimen.

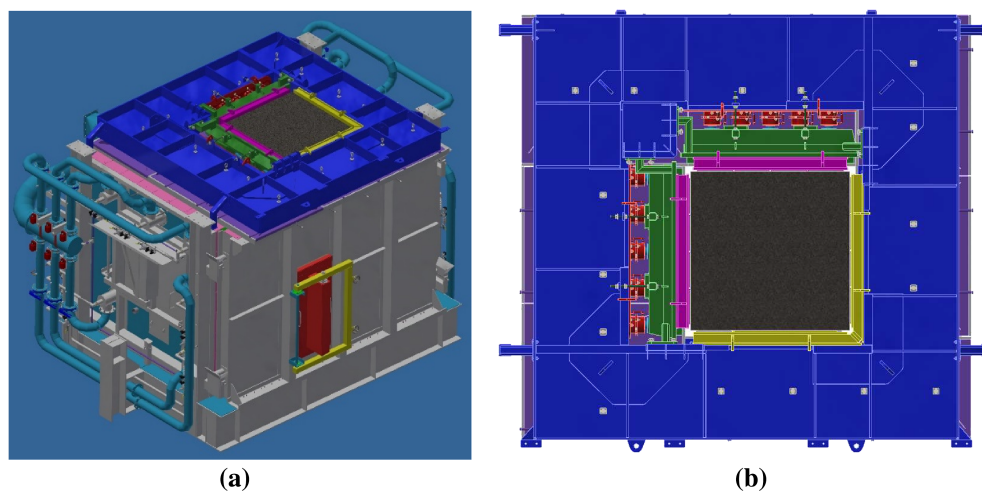
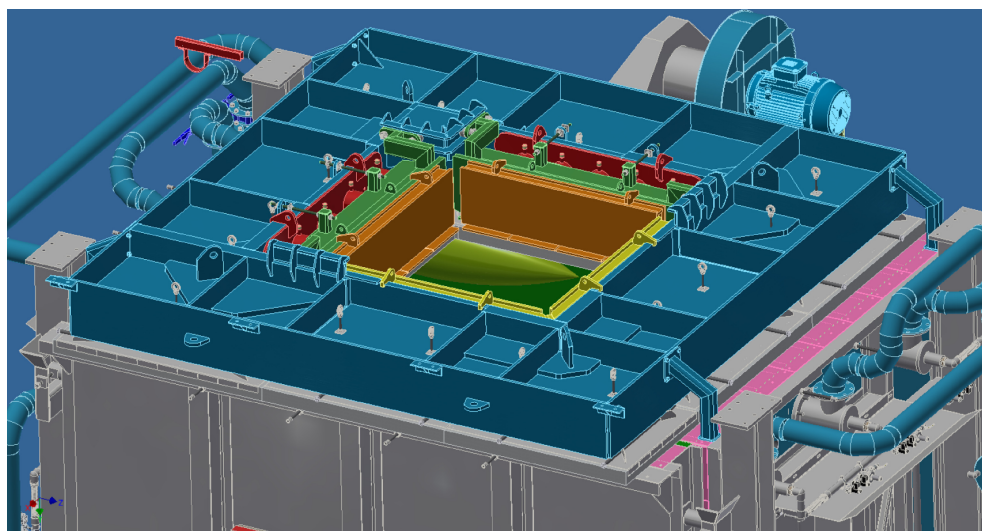


FIGURE 5 Schematic illustration of the biaxial rig structural frame exposure area.



shown in Figures 4 and 5 respectively. The self-reaction frame transmits the side loading via five horizontal hydraulics rams on one side (uniaxial loading) and two sides (biaxial loading). The load is monitored by three NATA Certified load cells (on each side) which are placed on the horizontal axis on two sides when needed. The side loading can either be applied and locked allowing the load to change as a function of time during the test or it can be helped via a programmable logic controller. The specimen is simply supported on four ledges which are 1550×30 mm yielding a fire-exposure area of 1490×1490 mm (approximately 2.2 m^2).

3.3 | Required testing standard and fire performance criteria for the rail tunnel lining

The flat panels were exposed to the German Tunnel-Lining Protection System fire according to the RABT

(Richtlinien für die Ausstattung und den Betrieb von Straßentunneln, also known as the ZTV tunnel curve [Zusätzlichen Technische Vertragsbedingungen] German Federal Ministry of Traffic, 1995, 1999, 2002) and the German Federal Railway Authority (Eisenbahn-Bundesamt [EBA]) curves.⁴ These curves differ from the standard, hydrocarbon and RWS time temperature curves as they include a cooling-off phase after 30 min (car) or 60 min (rail—see Figure 6). Beard and Carvel⁴ acknowledged the significance of a cooling-off stage and highlighted the works of Wetzig⁵⁴ who evaluated a concrete sample's resistance to heat through a test of concrete tunnel elements at the Hagerbach test gallery, Switzerland. Throughout the test, a concrete sample endured temperatures of up to 1600°C for 2 h with no signs of structural collapse, which only occurred after 30 min approximately of cooling whereby the sample exploded. This could occur during firefighting salvage operations within a tunnel whereby high-velocity water is applied on the affected structure, which can cause

concrete spalling due to high thermal shock.^{12,13} During the RABT ZTV (rail) time temperature curve, the furnace temperatures increase by 200°C per minute until 1200°C is reached. This temperature is then held for a further 55 min where then the furnace temperature decreases linearly for a duration of 115 min where it reaches temperatures below 90°C.¹⁸

General guidelines from AS1530.4:2014⁵² in relation to the build and size of the furnace were followed and concrete samples were manufactured and instrumented

in accordance with EFNARC 132F r3:2006.⁴¹ This standard specified the geometry of the specimen in addition to the position of the thermocouples that were cast. A total of 18 thermocouples were cast with each sample. The location of eight furnace control thermocouples was 100 mm from the underside of the unloaded flat specimens as required by EFNARC 132F r3:2006⁴¹ and AS1530.4:2014.⁵² The acceptance criterion for spalling was stipulated as the 95th percentile of the central area (800 × 800) as defined by EFNARC 132F r3:2006⁴¹ shall not suffer concrete spalling greater than 30 mm.

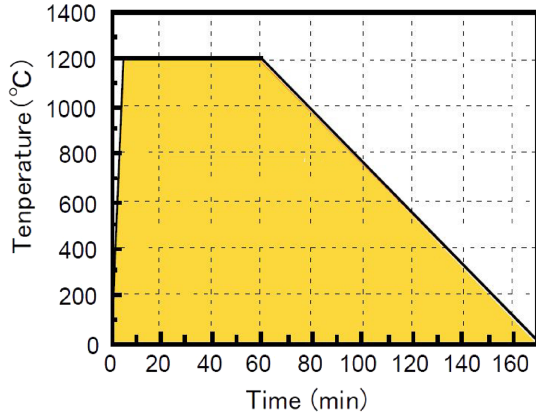


FIGURE 6 RABT ZTV (rail) temperature versus time curve (modified from ref. 43)

3.4 | Overview of the Metro Tunnel Project's specimens

A total of five unloaded flat panels (1550 × 1550 × 400 mm) were tested in this investigation. The specimens were cast on the 29th of October 2020 at the CYP D&C JV Project Logistics Yard (Flower Market) in West Melbourne, Victoria, Australia. The pour arrangement is shown in Figure 7. This figure also shows the location of the thermocouples, lifting lug arrangements and Specimen ID, which are referred to within this document. The details of the geometry and reinforcement of panels are shown in Figure 8. The reinforcement is consistent with N20 × 150 mm mesh,

PLATFORM LINING FIRE TEST PANELS POUR SETUP AND LABELLING

CONCRETE MIXES:

- MIX 1: NOT USED
- MIX 2: VS504MTER (1.6 kg/m3 PP Fibre)
- MIX 3: VS504MTER (1.4 kg/m3 PP Fibre)
- MIX 4: VS504MTER (1.2 kg/m3 PP Fibre)

PANEL LABEL: (MIX#, TYPE). Example: 1A

- A: For fire testing
- B: For fire testing
- C: Spare for fire testing
- D: For concrete coring

THERMOCOUPLE LABEL: (PANEL-T#)

Example: 1A-T1

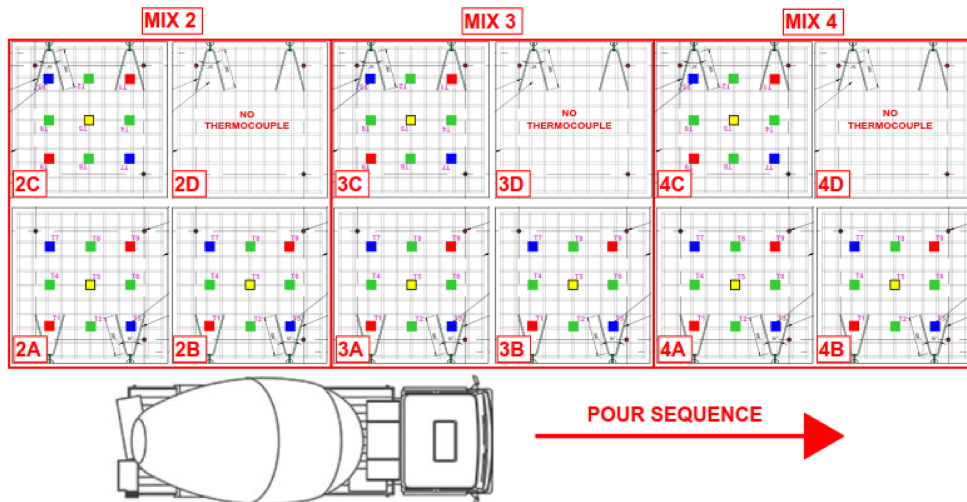
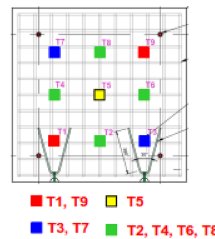


FIGURE 7 Specimen ID, details, and pour arrangement.

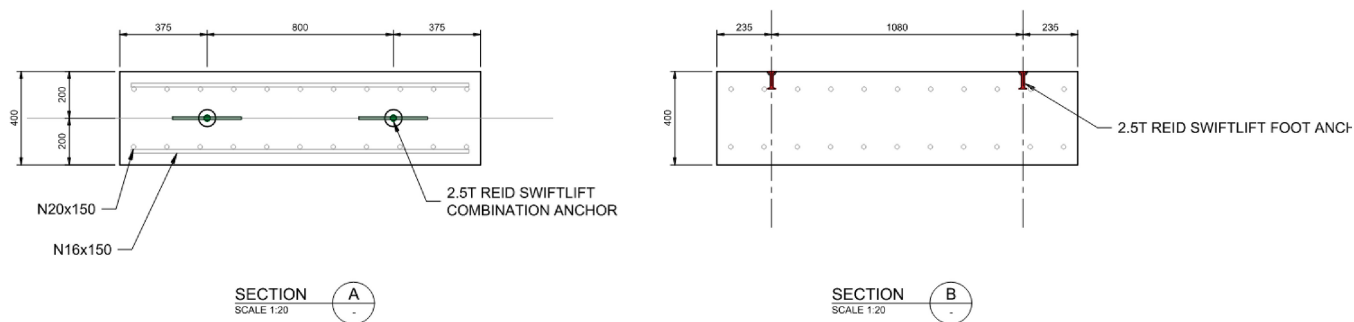


FIGURE 8 Reinforced panels geometry and reinforcement.

TABLE 3 Specimen ID and mix design.

Mix no		VS504MTER—1.4	VS504MTER—1.6	VS504MTER—1.2
Material		Mix design proportions		
GP cement	kg/m ³	158	158	158
Slag	kg/m ³	312	312	312
Amorphous silica	kg/m ³	10	10	10
14/10 mm agg	kg/m ³	1028	1028	1028
Natural sand	kg/m ³	508	508	508
Manufactured sand	kg/m ³	220	220	220
Type WR	kg/m ³	250–650/100	250–650/100	250–650/100
Type Re	kg/m ³	0–15/100	0–15/100	0–15/100
Type HWR	kg/m ³	300–700/100	300–700/100	300–700/100
Typical W/C ratio		0.40	0.40	0.40
Fiber dosage		1.4 kg/m ³	1.6 kg/m ³	1.2 kg/m ³
Fire panel ID		3A, 3B, 3C and 3D	2A, 2B, 2C and 2D	4A, 4B, 4C and 4D

50 mm from the top and bottom face and N16 × 150 bars. The mix design and specimen strength details along with their client ID are shown in Table 3. Limited details on the mix design can be provided due to intellectual property. Three different dosages of polypropylene fiber content were investigated (1.2, 1.4, and 1.6 kg/m³) whilst the base concrete mix was consistent. Although Eurocode 2²⁹ recommends a fiber dosage rate of at least 2.0 kg/m³, it has been shown by McNamee et al.²⁸ that reducing the dosage to 0.2 kg/m³ can reduce the spalling by 50% provide the aggregate is stable. Each mix design had a total of four specimens cast, two samples for fire testing, one extra backup specimen and one specimen for curing purposes prior to the fire test in alignment with EFNARC 132F r3:2006.⁴¹

3.5 | Specimen curing and conditioning regime

The curing required that the specimens were covered with heating blankets for 2 h after casting. After 3 days,

the specimens were transported to the Victoria University Structural Fire Testing Facility located in Werribee, Victoria, Australia, where they were placed in purpose built 40 ft shipping containers that were retrofitted to provide the require curing conditions. The specimens were cured for 28 days at 20 ± 2°C and at a relative humidity of greater than 90% ± 10%. After this initial curing period, the specimens were conditioned at 20 ± 2°C and at a relative humidity of greater than 95% ± 10% for 28 days followed by a further 56 days at 20 ± 2°C and at a relative humidity of greater than 50% ± 10%. The specimens were kept in these conditions, until the test date. The temperature and humidity control system were remotely monitored by mobile and the temperature and relative humidity curing profile are shown in Figures 9 and 10, respectively.

3.6 | Test setup and procedure

The fire testing program was carried out at the Victoria University, Werribee Campus, Institute for Sustainable

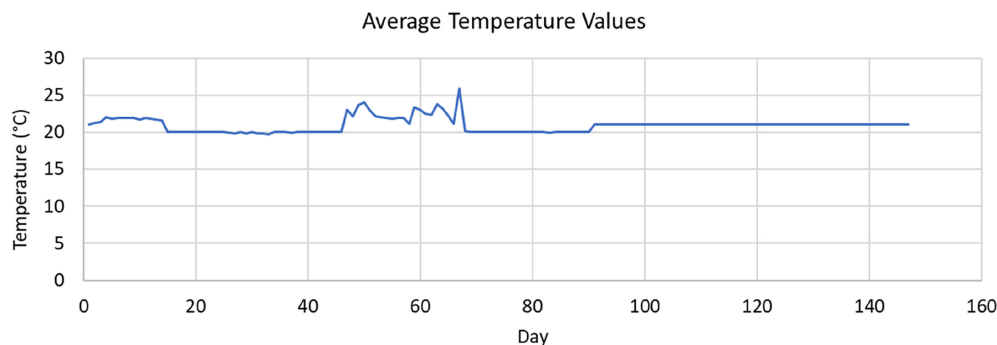


FIGURE 9 Average temperatures with curing container.

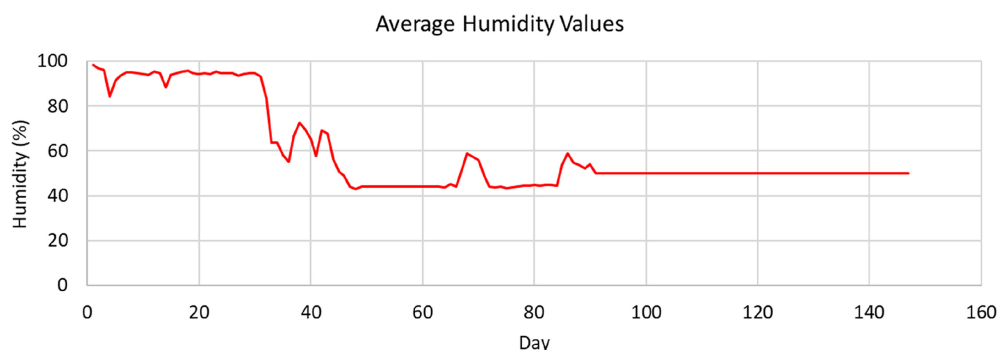


FIGURE 10 Average relative humidity with curing container.

TABLE 4 Specimen fire test details.

Fire test #	Test date	Specimen ID	Specimen age (days)	Dosage (kg/m ³)	Compressive strength (MPa) at test date	Moisture content average (%)
1	March 15, 2021	3C	137	1.4	60.0	6.1–6.4 ^a
2	March 18, 2021	2A	140	1.6	58.5	6.4
3	March 19, 2021	2B	141	1.6	58.5	6.4
4	March 29, 2021	4A	151	1.2	59.5	6.1
5	March 30, 2021	4B	152	1.2	59.5	6.1

^aNote, the moisture content of Specimen 3C was not recorded but given that it was cured identical to the other specimens, it is reasonable to assume the moisture content was between 6.1% and 6.4%.

Industries and Liveable Cities, Fire Engineering Division during March 2021. Five fire tests were carried out for the structurally loaded tunnel lining tests. Table 4 represents the summary of the fire test including the age of the concrete test panels.

The test setup was in accordance with the client specification, general fire testing requirements of AS1530.4:2014⁵² and EFNARC,⁴¹ which specified the location of the thermocouples and measurements required to be taken during the fire testing. Similar to the tests carried out previously,¹⁸ the furnace thermocouples were positioned 100 mm from the bottom of the specimen. A typical setup of the fire test is shown in Figure 11. The pooling of water on the unexposed surface commenced after approximately 30 min of fire exposure for all five tests carried out, which is consistent behavior

for these types of tests. This phenomenon was first reported by Woolson¹⁷ as noted by Jansson.¹⁵ The segments were loaded so that a uniformly distributed compressive stress equal to the maximum compression level of the fire-exposed surface of the actual tunnel structure was applied. The maximum compression level of the fire-exposed surface was determined to be 8 MPa and is based on the maximum design axial thrust in the tunnel lining. This stress level considers the ground and water pressure, the dead loads and restraint forces occurring during a fire event and the surrounding stiffness of the environmental soil. To achieve the desired loading, the specimen was loaded in a uniaxial configuration using five Enerpac 100 t rams and three 180 t loadcells. The uniaxial loading required to be applied was 506T but only 500T was able to be applied, presenting 98.8% of the

required loading due to the limitations of the system. Due to the imperfections of the loading and reaction surface, a 9 mm cement sheet was applied to ensure loading was transferred equally to the segment. The loadcells used were NATA calibrated with traceability to ISO17025. The loads were applied prior to the

commencement of the fire test in an alternative 10% increment until the maximum load was reached to avoid overstressing the specimen. The loads were then locked and monitored during the fire test. The detailed design of the structural testing rig is shown in Figure 12.

3.7 | *In situ* temperature instrumentation

EFNARC 132F r3:2006⁴¹ defines a central area of 800 × 800 mm where nine locations are specified where thermocouples are placed at varying depth as shown in Figure 13. The *in situ* thermocouples consist of Type K (NATA-certified up to 1200°C; 3-mm diameter, 310 stainless steel mineral insulated metal sheathed). A total of 18 thermocouples were cast for each flat panel apart from the panels that cores prior to the fire test were to be taken, as shown in Figure 14. The *in situ* thermocouples were located at 50 and 300 mm from the fire surface at location T1 and T9, 25 and 75 mm from the fire surface at location T2, T4, T6, and T8, 50 and 100 mm from the fire surface at location T3 and T7, and 75 plus 300 mm from the fire surface at location T5. The location and depths of the thermocouples are

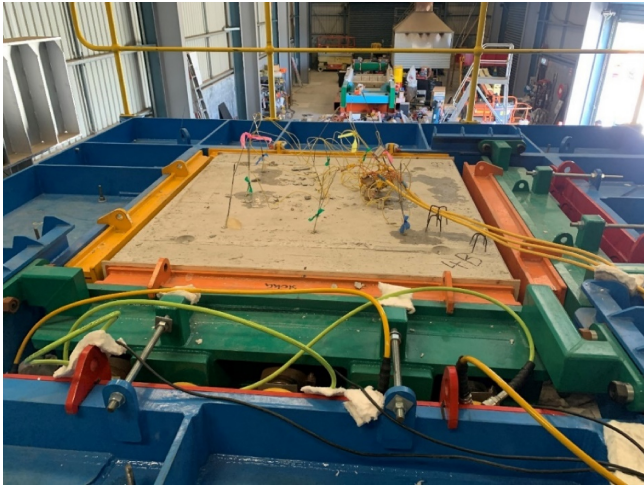


FIGURE 11 Photograph of the biaxial rig on top of the furnace.

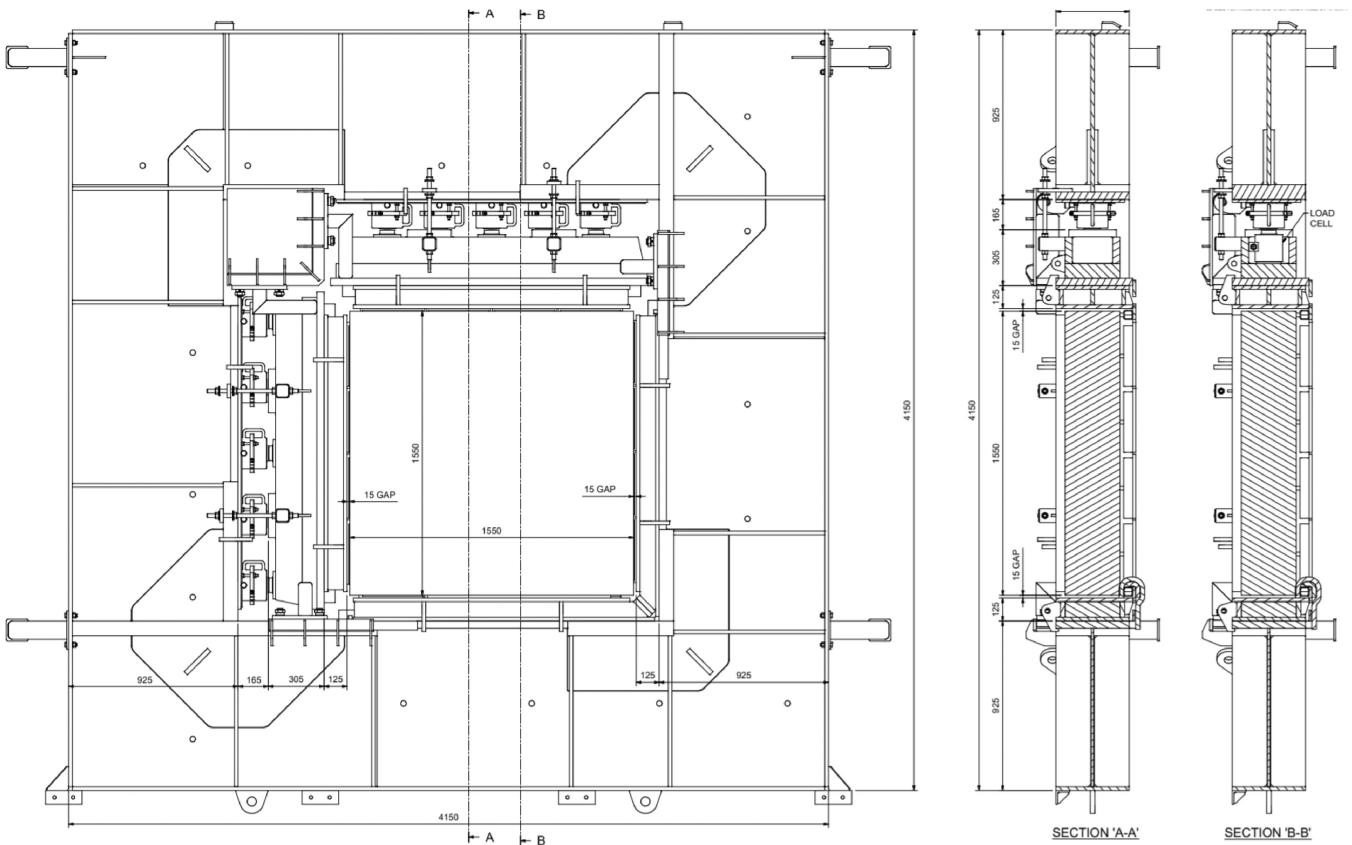


FIGURE 12 Structural testing rig design.

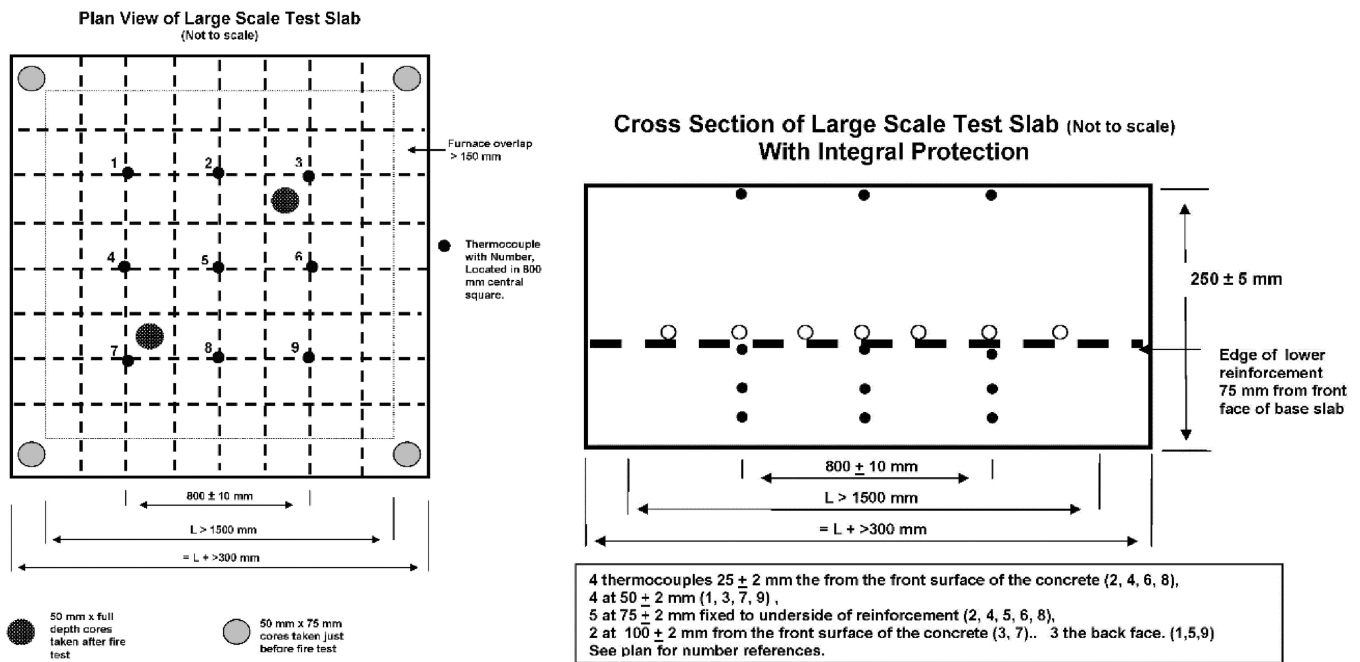


FIGURE 13 Specimens *in situ* thermocouple location in relation to EFNARC⁴¹ (extracted from EFNARC: 2006, Figures 3 and 4).

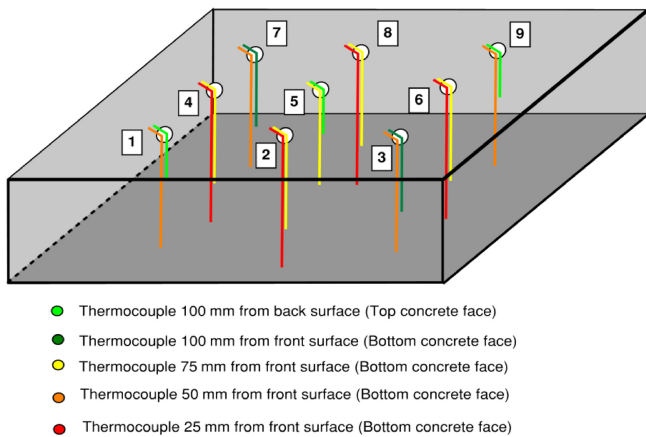


FIGURE 14 Schematic of the flat panel *in situ* thermocouple layout.

shown in Figure 14. An Agilent 34970a data logger was used to record the temperatures every 10 s for a period of 24 h.

4 | RESULTS AND DISCUSSION

4.1 | Furnace temperature versus time results

Figure 15 shows the furnace temperature versus time curve as measured by the eight control Type K thermocouples whilst Figure 16 represents the severity versus time of

the furnace. Both curves represent Fire Test 1, Specimen 4B. These data are similar across all fire tests (Specimens 3C, 2A, 2B, and 4A) and therefore they are not reproduced within this manuscript but are made available upon request. The data show that for all tests, the average furnace temperatures are in very close alignment to the required temperature given by the RABT ZTV (rail) requirements. The furnace severity was in alignment with the severity criterion for the duration of the test, as specified in Efectsis R0695 both the 2008⁵⁵ and 2020⁴⁸ versions. EFNARC⁴¹ defines the severity as measure of the percentage deviation in the area of the curve of the average temperature recorded by the specified furnace thermocouples versus time from the standard time–temperature curve.¹⁸ The computed area shall be calculated by the identical method, by the summation of areas at intervals not exceeding 1 min and shall be calculated above an axis of 0°C from time zero. As previously reported,¹⁸ as soon as spalling occurs, the temperatures of the furnace decrease and the lower limit if severity maybe breached. This is due to the fact that spalling causes virgin unexposed surfaces of the concrete to be exposed, which is accepted in accordance to Efectis 2020.⁴⁸

4.2 | *In situ* temperature versus time results

Figures 17–21 characterizes a collection of the *in situ* time temperature data at each thermocouple measurement depth and location for all the specimens. The

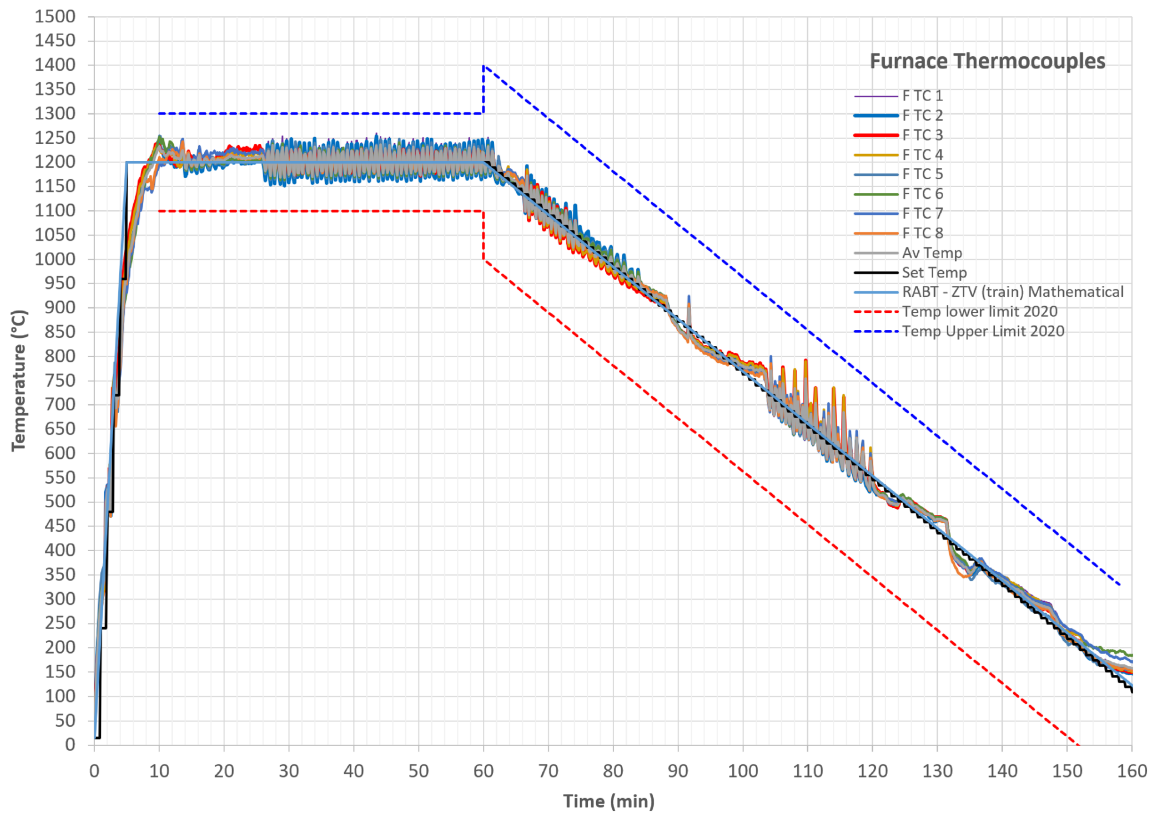


FIGURE 15 Temperature versus time for Specimen 4B.

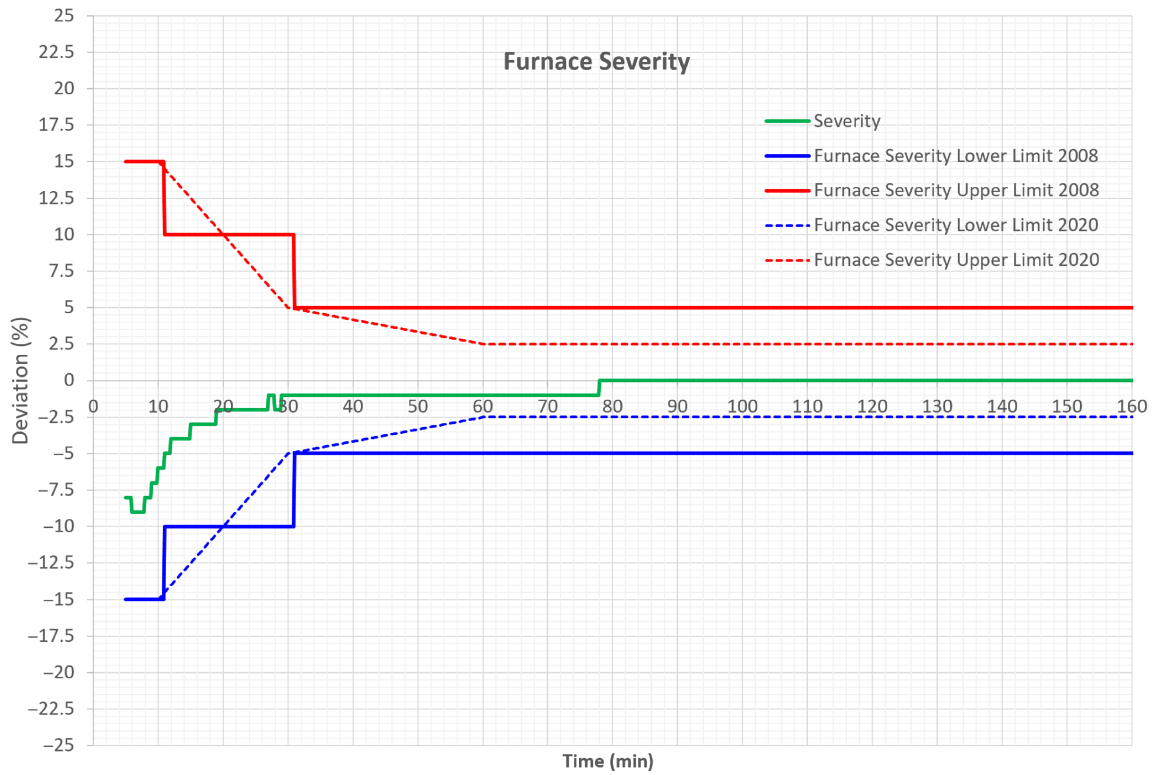


FIGURE 16 Furnace severity for Specimen 4B.

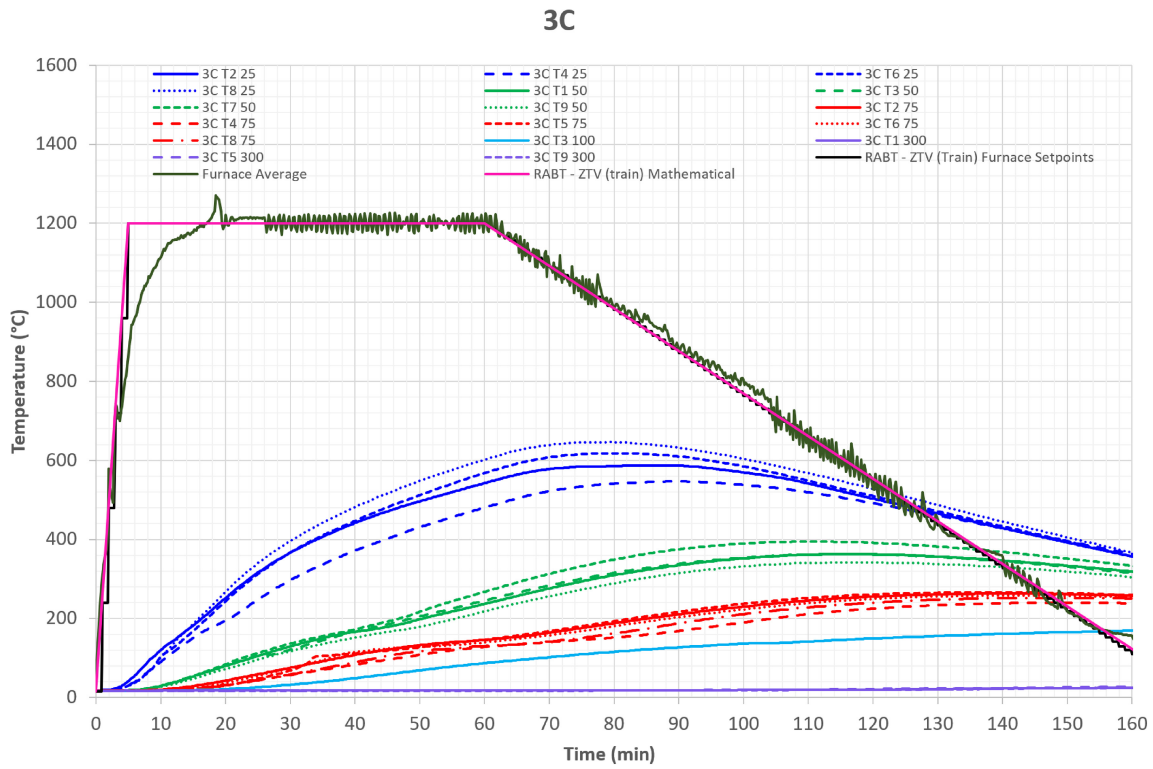


FIGURE 17 *In situ* time versus temperature measurements for Specimen 3C.

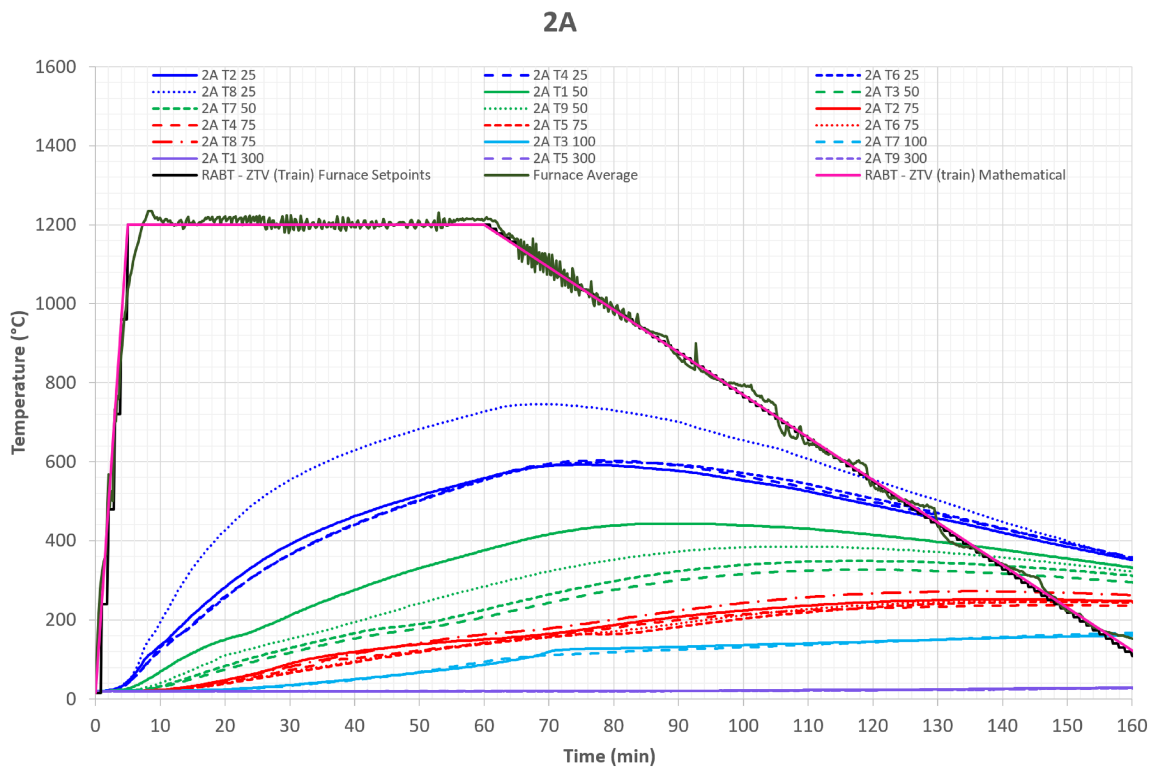


FIGURE 18 *In situ* time versus temperature measurements for Specimen 2A.

figures illustrate that the temperature profile follows the typical heat transfer between a hot and cold boundary as the *in situ* temperatures drops from the heated face

through to the non-heated face of the concrete panel.¹⁸ Note, the legend of each graph is represented as follows as previously detailed¹⁸:

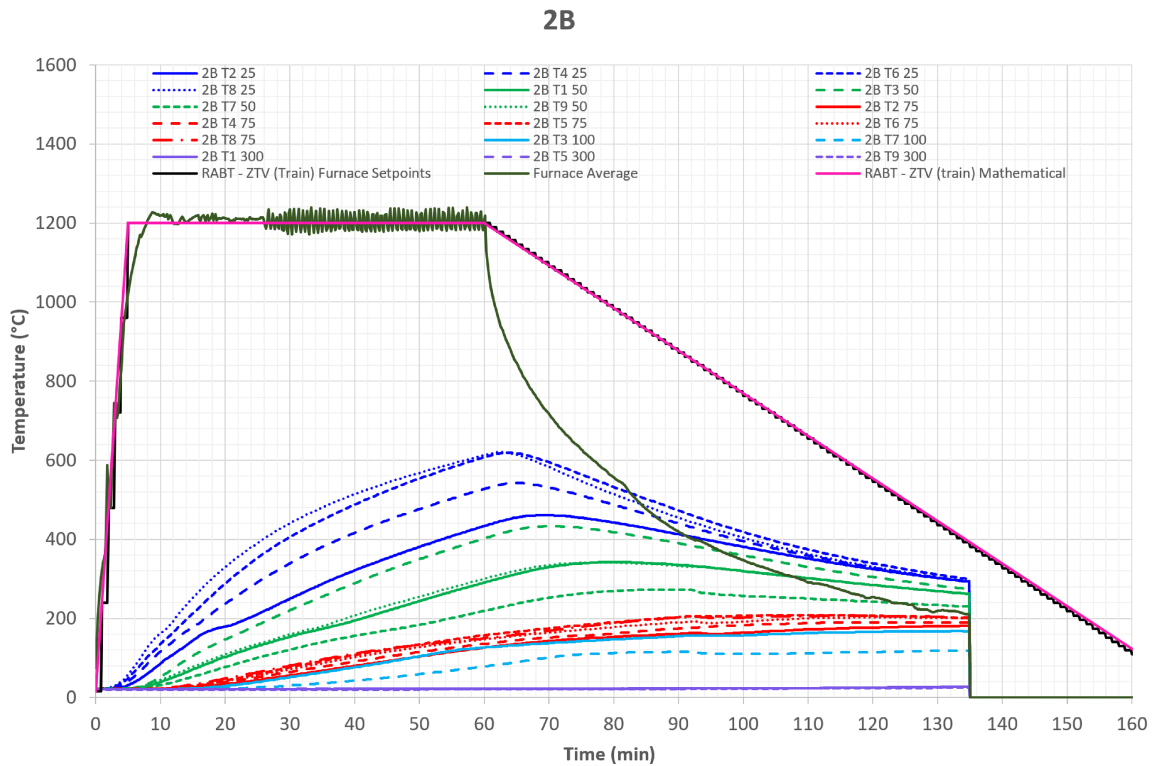


FIGURE 19 *In situ* time versus temperature measurements for Specimen 2B. Test was terminated at the conclusion of the heating phase (61 min) and no data was recorded after 134 min.

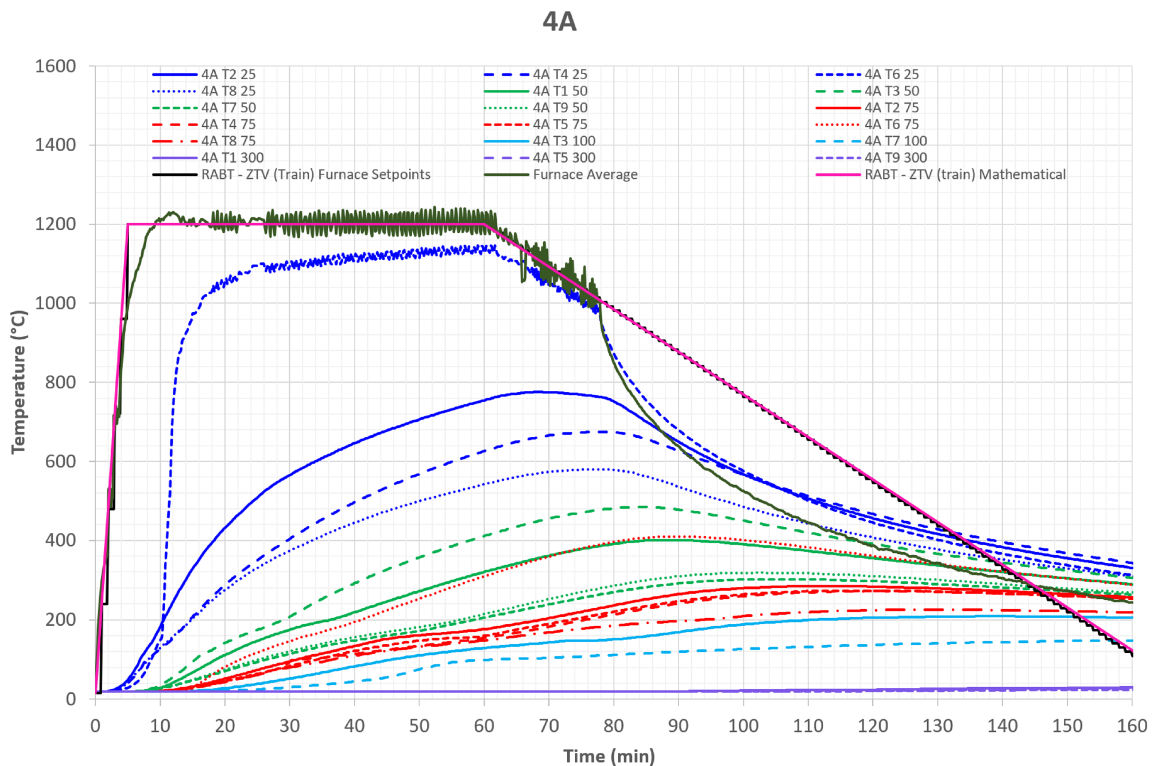


FIGURE 20 *In situ* time versus temperature measurements for Specimen 4A. Test was terminated at the conclusion of the heating phase and approximately 17 min during the cooling phase (77 min).

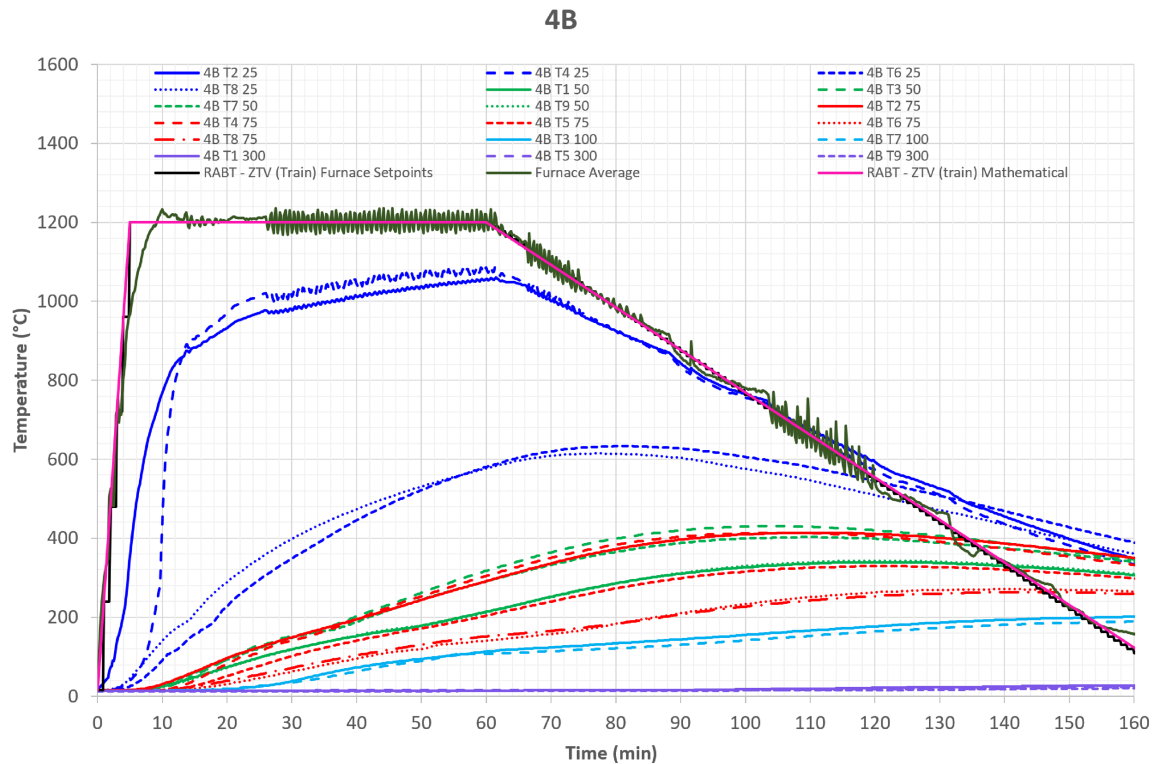


FIGURE 21 *In situ* time versus temperature measurements for Specimen 4B.

- T1 50—Represents a thermocouple embedded at location T1 at a depth of 50 mm from the heated face in accordance with the EFNARC procedure.
- T2 75—Represents a thermocouple embedded at location T2 at a depth of 75 mm from the heated face in accordance with the EFNARC procedure.
- T3 100—Represents a thermocouple embedded at location T3 at a depth of 100 mm from the heated face in accordance with the EFNARC procedure.
- T9 300—Represents a thermocouple embedded at location T9 at a depth of 300 mm from the heated face in accordance with the EFNARC procedure.

From Figure 20, Specimen 4A, one thermocouple located at T6 at a depth of 25 mm had a sharp temperature rise indicating that spalling occurs in this area. Given that the temperature did not asymptote to the furnace temperatures, this implies that at this location, spalling was confined to less than 25 mm. Similar findings can be seen in Figure 21, Specimen 4B, whereby at locations T2 and T4 at a depth of 25 mm, the *in situ* temperatures had a sharp temperature rise. The difference in spalling location for identical specimens is in alignment with the findings in the literature which state that there are discrepancies in spalling identical specimens and spalling is often sporadic in nature.^{18,56–60} In the third and fourth fire tests for Specimens 2B and 4A as shown in Figures 19 and 20, the test was terminated early, at the

start of the cooling phase due to the failure of the structural rig insulation, which could have jeopardized the loading frame. Given that spalling occurred within the first 30 min, the heating phase had completed, and no further spalling was noticed in Test 1, 2, and 5, so the early termination had no bearing on the results.

4.3 | Load applied versus time results

Figure 22 represents the structurally applied uniaxial horizontal load versus time profile for Specimen 4B. These data are similar across all loaded fire tests and therefore they are not reproduced within this manuscript but are made available upon request. The average total load is the average of the loads applied by the five hydraulic rams. The differences between the loads of these five rams were a maximum of 1.3%. The load was applied 30 min prior to the commencement of the furnace firing and was locked by means of a hydraulic manifold. The load was not required to be maintained during the testing procedure. As shown in Figure 21 the load steadily dropped to 95% at the conclusion of the test (160 min). This drop in load is postulated to be caused by a hydraulic oil leak even though the manifold was closed. This is explained by the fact that the hydraulic rams reached a maximum temperature of 41°C during the test which thinned out the oil and caused an oil leak.

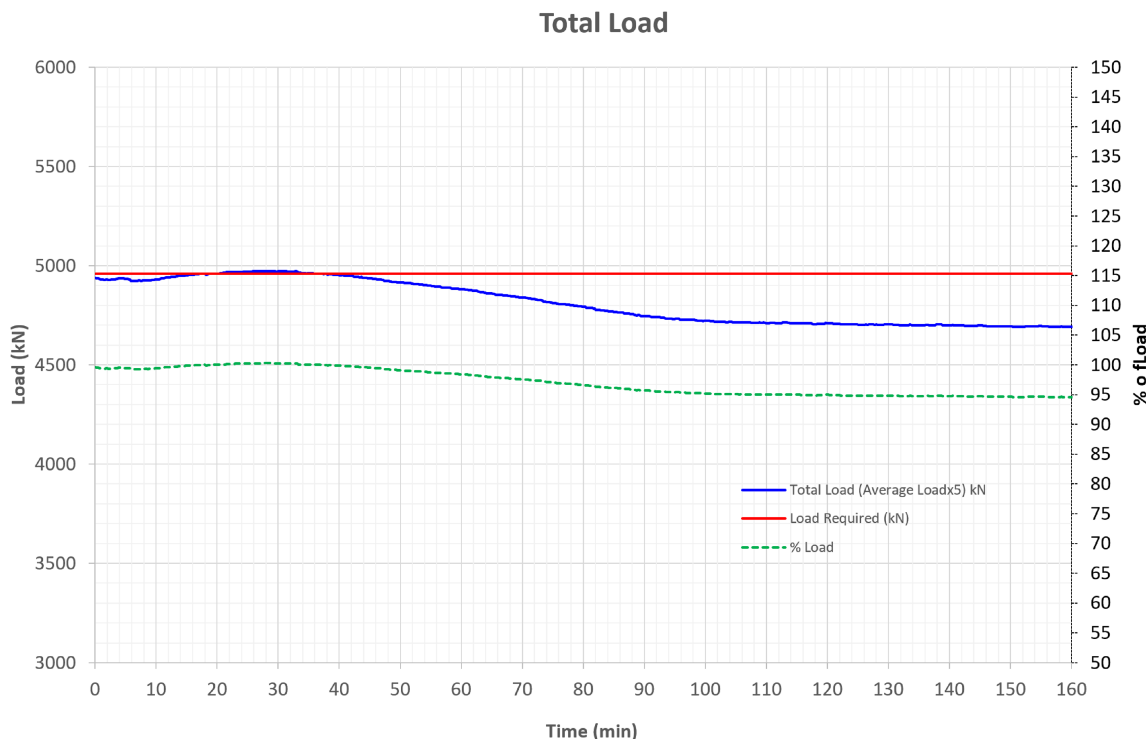


FIGURE 22 Structural load versus time for Specimen 4B.

TABLE 5 Summary of spalling results.

% Poly fibers	Specimen ID	Compressive strength at test date (MPa)	Mass loss kg	Mass loss %	Max spalling depth, 800 × 800 region (mm)	Approximate average depth, 800 × 800 region (mm)	Approximate average depth (entire fire-exposed region) (mm)	Spalling duration (min)
1.2	3C (1.4 kg/m ³)	60.0	55	2.25	17	-	-	Up to 15 min
1.4	2A (1.6 kg/m ³)	58.5	40	1.68	16.91	4.81	1.84	Up to 15 min
1.6	2B (1.6 kg/m ³)	58.5	50	2.10	25.91	5.52	3.44	Up to 15 min
1.6	4A (1.2 kg/m ³)	59.5	75	3.11	49.56	13.28	8.12	Up to 15 min
1.2	4B (1.2 kg/m ³)	59.5	90	3.73	47.18	20.00	10.96	Up to 15 min

Note: Specimen 3C did not undergo the surface scanning compared to the other specimens, the depths recorded were measured manually by digital calipers.

4.4 | Mass loss and degree of spalling

Table 5 denotes a summary of the spalling depths for the 800 × 800 mm central. Additionally, spalling measurements beyond the 800 × 800 is measured for comparative reasons. The spalling measurements were taken by an independent specialized contractor, Hi-tech Metrology, who operated a Creaform MetraSCAN3D to create a surface scan. The scan was done in a resolution of 2 mm with precision of 0.1 mm as per previous studies¹⁸ in order to generate spalling contour plots.

The scanning was performed post-coring, which explains the red circles on the spalling contour plots. The

specimen's passed based on the acceptance criteria which denotes the 95th percentile of the central area shall not endure concrete spalling more than 30 mm as per similar studies.¹⁸ No variation in the specimen exterior was observed between when the specimen was shifted from the furnace (approximately 24 h) and up to an interval of 3 days. Figures 23–27 represents photographs of the flat panels exposed surface after the fire test whilst Figures 28–31 represent the contour spalling plots of the flat panels after the fire test. A contour plot is not available for Specimen 3C.

The spalling criterion stipulated in this examination was centered on an average value which ought to be



FIGURE 23 Specimen 3C.



FIGURE 26 Specimen 4A.



FIGURE 24 Specimen 2A.



FIGURE 27 Specimen 4B.



FIGURE 25 Specimen 2B.

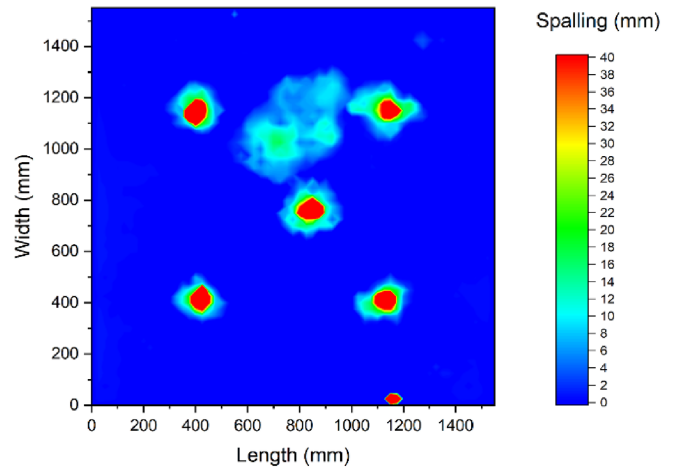


FIGURE 28 Panel 2A spalling contour plot (5.52 mm average spalling within 800 × 800 mm region).

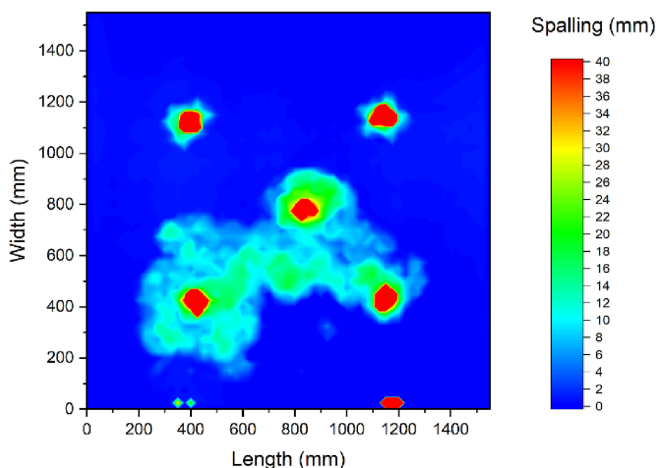


FIGURE 29 Panel 2B spalling contour plot (4.81 mm average spalling within 800 × 800 mm region).

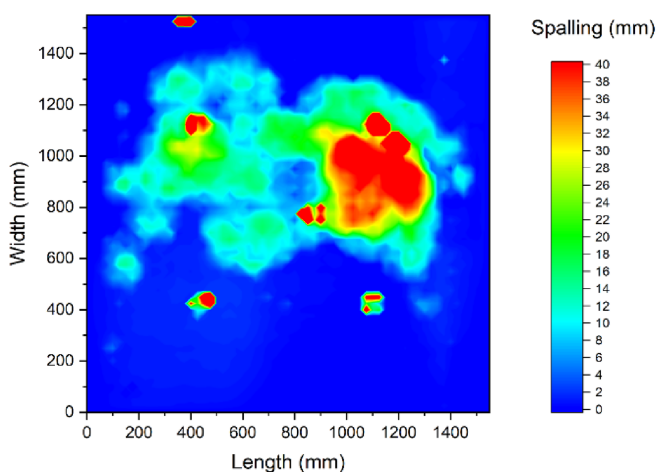


FIGURE 30 Panel 4A spalling contour plot (20.0 mm average spalling within 800 × 800 mm region).

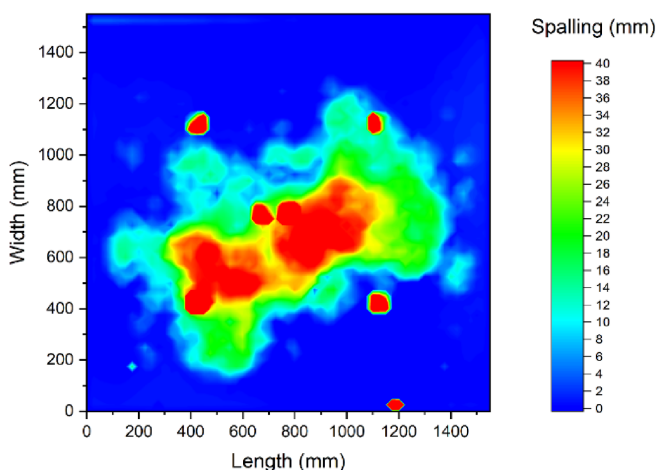


FIGURE 31 Panel 4B spalling contour plot (13.28 mm average spalling within 800 × 800 mm region).

implemented in the EFNARC 132F r3:2006⁴¹ testing guidelines which does not distinguish the spalling criterion. However, this is perhaps due to the fact that if a maximum spalling depth criterion was specified, it may turn out to be too rigorous.⁶¹ The test results showed that the concrete mix used performed well under combined structural and fire loading. This could be due to the high slag content of the mix design (66.3% of total cementitious material), which is known to have superior fire resistance compared to conventional 100% Portland Cement mix designs¹⁸ due to the phase changes of the hydration products.⁶² This is in addition to the aggregate being stable which is a significant factor in relation to concrete spalling.^{19,20} There was a clear relationship between polypropylene fiber dosage and concrete spalling. As shown in Table 5, at a polypropylene dosage rate of (1.2 kg/m³), the specimen mass loss was an average of 3.42% between two replicate panels (4A and 4B), compared to 2.25% for Specimen 3C (1.4 kg/m³) and 1.89% for the highest dosage specimens (1.6 kg/m³—2A and 2B). Whilst it has been reported by McNamee et al.²⁸ that reducing the dosage to 0.2 kg/m³ can reduce the spalling by 50% provided the aggregate is stable, the tests in that investigation were based on smaller samples under a lower loading scenario. In addition, it has been shown by Guerrieri and Fragomeni⁵⁹ that geometry and in particular specimen thickness influences the degree and magnitude of concrete spalling.

The results presented in this study are the only ones apart from those of Parwani et al.,⁴⁴ which tested large scale concrete panels in accordance with the procedures set out in EFNARC 132F r3:2006.⁴¹ It is postulated that the magnitude of spalling would have been significantly reduced if no load was applied to the segments. Comparisons to very similar mix design unloaded specimens (300 mm) exposed to the same testing program but in an unloaded state¹⁸ confirm this hypothesis. In those specimens, the spalling was on average less than 3 mm. These findings are in agreement to the works conducted by Bostrom et al.⁴² and Kodur and Phan⁶³ who demonstrated that mechanically loaded specimens are more prone to spalling during heating than unloaded specimens. Castillo⁶⁴ demonstrated that loaded specimens that were under sustained uniaxial load and heated exploded when the temperatures were between 320 and 360°C. In the investigational works overseen by Carré et al.,⁴⁷ it was displayed that no spalling occurred for slab specimens loaded up to 10 MPa but substantial exploding spalling happened at 15 MPa. No reason was provided for this observation. Contrary to this, Lo Monte et al.⁶⁵ demonstrated that explosive spalling happened at stress levels of 10 MPa. Miah et al.⁴⁶ revealed that spalling enhances as a function of applied stress level and is more definite when the samples are loaded biaxial than

uniaxial due to the orientation of the surface cracking which develops during heating.

It was hypothesized that the direction of the cracks (parallel to the heated surface in biaxial loading) are the ones that significantly increases the likelihood of spalling give that the pore pressure build-up cannot dissipate compared to vertical cracks to the surface when load is applied uniaxially. This could be the reasoning why the spalling was minimal in the tests conducted in this study and explain the pooling of water on the exposed surface as vertical surface cracking was evident to be clearly developing during the fire testing in all samples. As shown in Table 3, the moisture content of the specimens at the test date was between 6.1% and 6.4% which according to Hertz,⁶⁶ would have significantly increased the event of spalling and it is recommended to have moisture contents less than 3%. However, based on unpublished works by the author (Guerrieri) of this paper, the moisture content alone has negligible significance in relation to concrete spalling based on similar size flat panels submerged under water for over 100 days and taken out 4 h prior to being fire tested. In those tests, no spalling was observed due to the fact that the mix design was optimum (stable aggregate) and the polypropylene fiber content was in the order of 2.0 kg/m³. As stated by Khoury,⁶⁷ concrete spalling is a complex phenomenon reliant on a significant number of influencing parameters. The results offered here demonstrated that loading is one of the major considerations influencing spalling.

5 | CONCLUSIONS

This article presented for the first time a full-scale testing program and state-of-the-art structural testing rig capable of testing specimens up to 1800 × 1800 × 400 with either uniaxial or biaxial loading that met the requirements of EFNARC 132F r3:2006.⁴¹ Compared to previous published data, the results demonstrated that full-scale fire testing of concrete specimens under loading provides a valid and exact representation, whilst unloaded specimens lead to conservative and inaccurate results. The test setup used for this study was the only one of its kind in Australia which integrates structural loading and appropriate boundary conditions for the analysis of the platform tunnel side wall and arch lining in the State Library and Town Hall stations for structural stability for the duration of a serious fire event. The testing contributed to delivering fire safety confidence for the project to satisfy obligations under the RSNL framework.

Whilst spalling was observed in all the specimens which was categorized as surface spalling, it is speculated that the scale of spalling would have been considerably

reduced if no load was applied to the segments. Additionally, it is believed that the vertical cracking that was generated during combined structural and fire loading allowed the mitigation of water, which was observed on the unexposed surface that helped reduce the magnitude of spalling.

The in-depth analysis showed that at some locations, the temperatures at 25 mm spiked for Specimens 4A and 4B (1.2 kg/m³), which was in alignment with the general trend observed, the spalling mass loss increased as the polypropylene fiber dosage decreased. However, given that the spalling patterns were random, the location of the maximum depths were different between identical specimens, it is difficult to draw any further conclusions. In all fire tests, the water pooling phenomenon on the unexposed side was witnessed, at around after 30 min into the fire test. This was caused by a combination of the sweating of the specimens and the vertical cracking which developed in the specimens and provided a pathway for the water to migrate to the surface away for the heat exposure. Initially postulated by Woolson¹⁷ and still accepted today, the water pooling is either associated with free water contained by the specimen that is driven by mechanical means or crystallization disassociated by the heat exposure. As stated by Jansson and Boström⁶⁸ and confirmed by Guerrieri,¹⁸ the mechanism and reason of the pooling of water needs to be revealed if an accurate numerical model for concrete spalling is to be established.

AUTHOR CONTRIBUTIONS

All authors equally contributed to this manuscript. All authors have read and agreed to the published version of the manuscript.

ACKNOWLEDGMENTS

The authors wish to acknowledge the support of all technical staff at Victoria University, members of the Metro Tunnel Project, Rail Projects Victoria and Furnace Engineering Australia. Open access publishing facilitated by Victoria University, as part of the Wiley - Victoria University agreement via the Council of Australian University Librarians.

CONFLICT OF INTEREST STATEMENT

The authors declare no conflict of interest.

DATA AVAILABILITY STATEMENT

The data that support the findings of this study are available from the corresponding author upon reasonable request.

ORCID

Maurice Guerrieri  <https://orcid.org/0000-0001-7916-7003>

REFERENCES

- Khouri G, Majorana CE, Pesavento F, Schrefler BA. Modelling of heated concrete. *Mag Concr Res.* 2002;54(2):77–101.
- Yan Z-G, Shen Y, Zhu H-H, Li X-J, Lu Y. Experimental investigation of reinforced concrete and hybrid fibre reinforced concrete shield tunnel segments subjected to elevated temperature. *Fire Saf J.* 2015;71:86–99.
- Zhang X, Wu X, Park Y, Zhang T, Huang X, Xiao F, et al. Perspectives of big experimental database and artificial intelligence in tunnel fire research. *Tunn Undergr Space Technol.* 2021;108:103691.
- Beard A, Carvel R. *The handbook of tunnel fire safety.* London: ICE; 2012.
- Hua N, Tessari A, Elhami Khorasani N. Characterizing damage to a concrete liner during a tunnel fire. *Tunn Undergr Space Technol.* 2021;109:103761.
- Lacroix D. Managing road tunnel safety: Today's challenge. In: *Proceedings from the Third International Symposium on Tunnel Safety and Security, Stockholm, Sweden, March 12–14. 2008.*
- Siemon M, Zehfuß J. Behavior of structural tunnel elements exposed to fire and mechanical loading. *J Struct Fire Eng.* 2019;9(2):138–46.
- Wasantha P, Guerrieri M, Xu T. Effects of tunnel fires on the mechanical behaviour of rocks in the vicinity – a review. *Tunn Undergr Space Technol.* 2020;108:103667.
- Maraveas C, Vrakas AA. Design of concrete tunnel linings for fire safety. *Struct Eng Int.* 2018;24(3):319–29.
- Wu Y. *The handbook of tunnel fire safety, a Beard, R Carvel, Thomas Telford ltd.* London: Elsevier; 2005. ISBN:0727731688.
- Ulm F-J, Acker P, Lévy M. The “Chunnel” fire. II: analysis of concrete damage. *J Eng Mech.* 1999;125(3):283–9.
- Sakkas K, Vagiokas N, Tsiamouras K, Mandalozis D, Benardos A, Nomikos P. In-situ fire test to assess tunnel lining fire resistance. *Tunn Undergr Space Technol.* 2019;85:368–74.
- Jönsson J. HGV traffic—consequences in case of a tunnel fire. In: *Proceedings from the Fourth International Symposium on Tunnel Safety and Security, Frankfurt am Main, Germany, March 17–19. 2010.*
- Helene P, Britze C, Carvalho M. Fire impacts on concrete structures. A brief review. *Rev ALCONPAT.* 2019;10(1):1–21.
- Jansson R. Fire spalling of concrete – a historical overview. *MATEC Web Conf.* 2013;6:01001.
- Barret I. On the French and other methods of constructing iron floors. *Civil Eng Archit J.* 1854;XVII:5–9.
- Woolson IH. Investigation of the effect of heat upon the crushing strength and elastic properties of concrete. In: *Proceedings of the American Society for Testing Materials, Philadelphia, PA. 1905.*
- Guerrieri M, Sanabria C, Lee WM, Pazmino E, Patel R. Design of the metro tunnel project tunnel linings for fire testing. *Struct Concr.* 2020;21(6):2452–80.
- Mohd Ali A, Sanjayan J, Guerrieri M. Effect of aggregate size on the spalling of high-strength wall panels exposed to hydrocarbon fire. *J Mater Civil Eng.* 2017;29(12):04017237.
- Mohd Ali A, Sanjayan J, Guerrieri M. Specimens size, aggregate size, and aggregate type effect on spalling of concrete in fire. *Fire Mater.* 2018;42(1):59–68.
- Ali AM, Sanjayan J, Guerrieri M. Performance of geopolymer high strength concrete wall panels and cylinders when exposed to a hydrocarbon fire. *Construct Build Mater.* 2017;137:195–207.
- Guerrieri M, Sanjayan JG. Behavior of combined fly ash/slag-based geopolymers when exposed to high temperatures. *Fire Mater.* 2010;34(4):163–75.
- Guerrieri M, Sanjayan J, Collins F. Residual strength properties of sodium silicate alkali activated slag paste exposed to elevated temperatures. *Mater Struct.* 2010;43(6):765–73.
- Guerrieri M, Sanjayan J, Collins F. Residual compressive behavior of alkali-activated concrete exposed to elevated temperatures. *Fire Mater.* 2009;33(1):51–62.
- Li Y, Pimienta P, Pinoteau N, Tan KH. Effect of aggregate size and inclusion of polypropylene and steel fibers on explosive spalling and pore pressure in ultra-high-performance concrete (UHPC) at elevated temperature. *Cem Concr Compos.* 2019;99:62–71.
- Liu X, Ye G, de Schutter G, Yuan Y, Taerwe L. On the mechanism of polypropylene fibres in preventing fire spalling in self-compacting and high-performance cement paste. *Cem Concr Res.* 2008;38(4):487–99.
- Xiao JZ, Falkner H. On residual strength of high-performance concrete with and without polypropylene fibres at elevated temperatures. *Fire Saf J.* 2006;41(2):115–21.
- McNamee R, Sjöström J, Boström L. Reduction of fire spalling of concrete with small doses of polypropylene fibres. *Fire Mater.* 2021. n/a(n/a);45:943–51.
- EN 1992-1-2. Eurocode 2: Design of concrete structures—Part 1–2: general rules—structural fire design; authority: the European Union per regulation 305/2011, directive 98/34/EC, directive 2004/18/EC; European Union: Brussels, Belgium. 2004.
- McNamee R. Fire spalling theories – realistic and more exotic ones. In: *Proceedings of the 6th International Workshop on Concrete Spalling due to Fire Exposure, Sheffield, UK. 2019.*
- Yan Z-G, Zhu H-H, Ju JW, Ding W-Q. Full-scale fire tests of RC metro shield TBM tunnel linings. *Construct Build Mater.* 2012;36:484–94.
- Yan Z, Shen Y, Zhu H, Lu Y. Experimental study of tunnel segmental joints subjected to elevated temperature. *Tunn Undergr Space Technol.* 2016;53:46–60.
- Richter E. Fire test on single-shell tunnel segments made of a new high-performance fireproof concrete. In: *Workshop: Fire Design of Concrete Structures: What Now. 2005.*
- Haack A. Fire protection in traffic tunnels: general aspects and results of the EUREKA project. *Tunn Undergr Space Technol.* 1998;13(4):377–81.
- Haack A. Fire protection in traffic tunnels—initial findings from large-scale tests. *Tunn Undergr Space Technol.* 1992;7(4):363–75.
- Yasuda F, Ono K, Otsuka T. Fire protection for TBM shield tunnel lining. In: *Proceedings of the 30th ITA-AITES World Tunnel Congress Singapore, May 22–27. 2004.*
- Kaundinya I, Dehn F, Nause P, Juknat M. Fire tests at large-scale specimens of ZTV-ING conform fiber-modified concrete for inner shells of road tunnels. In: *Proceedings of 1st International Workshop on Concrete Spalling due to Fire Exposure, Leipzig. 2009.*
- Caner A, Böncü A. Structural fire safety of circular concrete railroad tunnel linings. *J Struct Eng.* 2009;135(9):1081–92.
- Boxheimer S, Knilt J, Dehn F. Fire test on precast tunnel segments for the Liefkenshoekspoortunnel in Antwerp. In: *Workshop Proceedings: “spalling on concrete due to fire exposure,” Leipzig. 2009.*
- Lönnermark A. *On the characteristics of fires in tunnels.* Lund: Lund University; 2005.

41. EFNARC. Specification and guidelines for testing of passive fire protection for concrete tunnels linings. Switzerland: European Federation of National Associations Representing Concrete; 2006. p. 1–27.
42. Boström L, Wickström U, Adl-Zarrabi B. Effect of specimen size and loading conditions on spalling of concrete. *Fire Mater.* 2007;31(3):173–86.
43. Kato M, Dobashi H, Tajima H, Kawada N, Takahama T. The application of fireproof SFRC segments and cast-in-place fireproof concrete to metropolitan expressway Yokohama circular northern route. ME Obayashi Corporation. 2015.
44. Parwani K, Bienefeld J, Rakovec T, Haring F. Fire behaviour of large scale loaded tunnel segment tests for project Rotterdamsebaan, The Netherlands. IABSE Congress, Ghent 2021: Structural Engineering for Future Societal Needs. 2021.
45. Lo Monte F, Felicetti R, Meda A, Bortolussi A. Assessment of concrete sensitivity to fire spalling: a multi-scale experimental approach. *Construct Build Mater.* 2019;212:476–85.
46. Miah MJ, Monte FL, Felicetti R, Carré H, Pimienta P, La Borderie C. Fire spalling behaviour of concrete: role of mechanical loading (uniaxial and biaxial) and cement type. *Key Eng Mater.* 2016;711:549–55.
47. Carré H, Pimienta P, la Borderie C, Pereira F, Mindeguia JC. Effect of compressive loading on the risk of spalling. *MATEC Web Conf.* 2013;6:01007.
48. Efectis. Test procedure for fire-resistant tunnel lining and other tunnel components. Utrecht: Rijkswaterstaat Ministry of Infrastructure and the Environment; 2020.
49. Hua N, Khorasani NE, Tessari A, Ranade R. Experimental study of fire damage to reinforced concrete tunnel slabs. *Fire Saf J.* 2021;127:103504.
50. Taillefer N, Pimienta P, Dhima D. Spalling of concrete: a synthesis of experimental tests on slabs. *MATEC Web Conf.* 2013; 6:01008.
51. National Transport Commission. Meaning of duty to ensure safety so far as is reasonably practicable–SFAIRP. The Office of Rail Safety Regulator. 2016. <https://nraspricms01.blob.core.windows.net/assets/documents/Guideline/Guideline-Meaning-of-Duty-to-Ensure-Safety-SFAIRP-May-2021.pdf>. Accessed 17 Nov 2023.
52. Standards Australia. Methods for fire tests on building materials, components and structures fire-resistance tests for elements of construction, in AS1530.4. 2014, Australia: Standards Australia.
53. Standards Australia. AS 3600: 2018 concrete structures. Sydney: Standards Australia Limited; 2018.
54. Wetzig V. Destruction mechanisms in concrete material in case of fire, and protection systems. In: Proceedings of the Fourth International Conference on Safety in Road and Rail Tunnels, held Madrid, Spain, April 2–6. 2001.
55. Efectis. Fire testing procedure for concrete tunnel linings and other tunnel components. The Netherlands: Rijkswaterstaat Ministry of Infrastructure and the Environment; 2008.
56. Phan LT, Carino NJ. Review of mechanical properties of HSC at elevated temperature. *J Mater Civ Eng.* 1998;10(1):58–64.
57. Phan LT, Carino NJ. Fire performance of high strength concrete: research needs. Gaithersburg, MD: Advanced Technology in Structural Engineering; 2000. p. 1–8.
58. Phan LT, Lawson JR, Davis FL. Heating, spalling characteristics and residual properties of high performance concrete. In: UJNR Panel on Fire Research and Safety. 2000.
59. Guerrieri M, Fragomeni S. Mechanisms of spalling of concrete panels of different geometry in hydrocarbon fire. *J Mater Civ Eng.* 2016;28(12):04016164.
60. Guerrieri M, Fragomeni S. Spalling of large-scale walls exposed to a hydrocarbon fire. *J Mater Civ Eng.* 2019;31(11):04019249.
61. Monckton H. Practical design, testing & verification guidelines for pre-cast segmental tunnel linings subjected to fire loading. *Tunn Undergr Space Technol.* 2018;77:237–48.
62. Mendes A, Sanjayan J, Collins F. Phase transformations and mechanical strength of OPC/slag pastes submitted to high temperatures. *Mater Struct.* 2008;41(2):345–50.
63. Kodur V, Phan L. Critical factors governing the fire performance of high strength concrete systems. *Fire Saf J.* 2007;42(6–7):482–8.
64. Castillo C, Durrani AJ. Effect of transient high temperature on high-strength concrete. *Mater J.* 1990;87(1):47–53.
65. Lo Monte F, Rossino C, Felicetti R. Spalling test on concrete slabs under biaxial membrane loading. In: 4th International Workshop on “Concrete Spalling due to Fire Exposure”. 2015.
66. Hertz KD. Limits of spalling of fire-exposed concrete. *Fire Saf J.* 2003;38(2):103–16.
67. Khoury GA, Anderberg Y. Fire safety design – concrete spalling review. Report submitted to Swedish National Road Administration. 2000.
68. Jansson R, Boström L. Fire spalling – the moisture effect. In: 1st International Workshop on Concrete fire Spalling due to Fire Exposure. 2009.

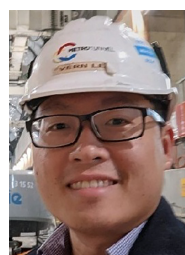
AUTHOR BIOGRAPHIES



Maurice Guerrieri, Institute of Sustainable Industries & Liveable Cities (ISILC), Victoria University, Melbourne, Victoria, Australia.
Email: maurice.guerrieri@vu.edu.au.



Duffy Lee, Gamuda Australia.
Email: pakhin.lee@glcwp.com.au.



Vern Lee, Love Reinforcing, Braybrook, Victoria, Australia.
Email: vern.lee@lovereinforcing.com.au.



Luke Haines, Riscoconsult.
Email: luke@riscoconsult.com.

How to cite this article: Guerrieri M, Lee D, Lee V, Haines L. Effect of uniaxial loading on the spalling of concrete panels for Melbourne's Metro Tunnel Project. *Structural Concrete*. 2024;25(3): 1676–701. <https://doi.org/10.1002/suco.202200556>